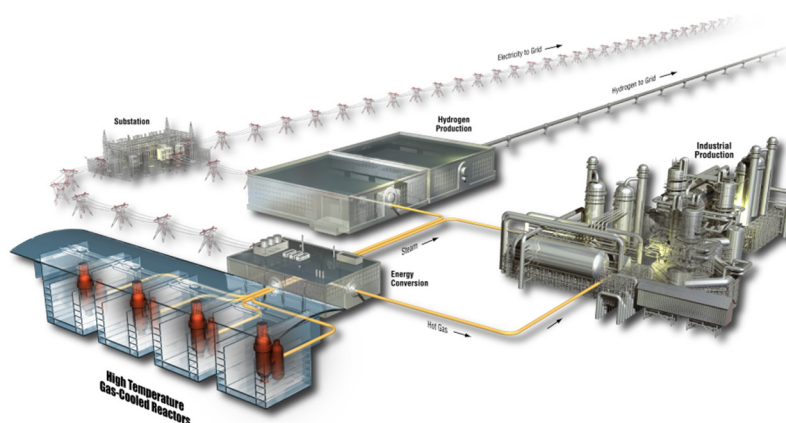# Assessment of Material Properties for TRISO Fuel Particles used in PARFUME

William F. Skerjanc
Blaise P. Collin

August 2018

INL
Idaho National Laboratory

Assessment of Material Properties for TRISO Fuel Particles used in PARFUME

William F. Skerjanc
Blaise P. Collin

August 2018

INL ART Program

Assessment of Material Properties for TRISO Fuel Particles used in PARFUME

INL/EXT-18-44631
Revision 0

August 2018

Author:

_____   8/1/2018
William F. Skerjanc   Date
Technical Lead, TRISO Fuel Performance Modeling

Technical Reviewer: (Confirmation of mathematical accuracy, and correctness of data and appropriateness of assumptions.)

_____   8/1/18
David A. Petti   Date
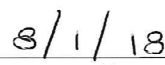Technical Reviewer

Approved by:

_____   8/1/18
Paul A. Demkowicz   Date
AGR Fuels Director

_____   8/1/18
Michelle T. Sharp   Date
INL Quality Engineer

SUMMARY

The purpose of this study is to identify the material properties that have the largest impact on the failure probability of tristructural isotropic (TRISO)-coated fuel particles under irradiation. For the most part, these material properties were obtained from experimental data of historical TRISO fuel-development programs in Europe and the United States. The adequacy of these historical constitutive material properties is being evaluated as part of the Advanced Gas Reactor Fuel Development and Qualification Program. The TRISO fuel performance modeling code PARFUME was used to assess the material properties that have the main influence on the probability of failure of the silicon carbide (SiC) layer of TRISO fuel particles. Although some of these material properties exhibit a large variability according to published data, only a few of them have a significant impact on the SiC failure probability, namely the irradiation-induced creep and dimensional change of the inner pyrolytic carbon layer.

CONTENTS

FIGURES

TABLES

ACRONYMS

AGR	Advanced Gas Reactor
BAF	Bacon Anisotropy Factor (degree of anisotropy)
BNFL	British Nuclear Fuels Ltd
CEA	Commissariat à l'énergie atomique et aux énergies alternatives
CEGA	Combustion Engineering General Atomics
EFPD	effective full power day
FIMA	fissions per initial (heavy) metal atom
FZJ	Forschungszentrum Jülich
HTR	high temperature reactor
INL	Idaho National Laboratory
IPyC	inner pyrocarbon
LWR	light water reactor
MATPRO	library of material properties for LWR accident analysis
PIE	post-irradiation examination
OPyC	outer pyrocarbon
PARFUME	particle fuel model
SiC	silicon carbide
SMF	sensitivity multiplication factor
TRISO	tristructural isotropic
UCO	uranium oxycarbide
UO_2	uranium dioxide

NOMENCLATURE

B_u burnup (%FIMA)

E   neutron energy (MeV)

Φ fast neutron fluence ($\times 10^{25}$ n/m^2, E >0.18 MeV)

ρ density (g/cm^3)

T   temperature (°C or K)

The temperature and density applies to the material (kernel, buffer, PyC, or SiC) under consideration, unless specified otherwise.

Notes

1. Material properties are detailed in the report *NP-MHTGR material models of pyrocarbon and pyrolytic silicon carbide* (hereafter referred to as the CEGA report) by the Combustion Engineering General Atomics Corporation (CEGA, 1993) and in the *PARFUME Theory and Model Basis Report* (Miller et al., 2009).

2. Due to limited information of specific material property behavior at high fast fluence, most material properties have a cut-off at a fast-fluence value of 4×10^{25} n/m^2 (E >0.18 MeV). For fast fluences higher than the cut-off, material properties keep their value at the cut-off. However, most high temperature gas-cooled reactors are designed with peak fast fluences at or below these levels.

3. Parameter-dependent material properties extracted from literature data correspond to properties at the same fuel parameter values (density, etc.) as used in this study (see Table 1).

4. Many material-property values and correlations found in the literature depend on fast-neutron fluence. Historically, researchers have used different fast neutron fluence energy level cutoffs in their data. For consistency, all data have been converted to correspond to fast fluence with neutron energy larger than 0.18 MeV. The ratio of fast-fluence spectrum with neutron energy larger than 0.18 MeV to fast-fluence spectrum with neutron energy larger than 0.1 MeV is taken equal to 0.91.

Assessment of Material Properties for TRISO Fuel Particles in PARFUME

1. INTRODUCTION

Tristructural isotropic (TRISO) particles have been designed since the 1960s as the preferred fuel technology for use in high-temperature gas-cooled reactors. These fuel particles are characterized by superior fission-product containment capability up to temperatures reached in the worst accident scenarios.

Coated-particle fuel consists of spherical kernels—less than a millimeter in diameter—of oxide, carbide, or oxycarbide (a mixture of oxide and carbide) fuel encased in multiple coating layers: a porous carbon buffer, a dense inner layer of pyrolytic carbon (IPyC), a silicon carbide (SiC) layer, and an outer pyrolytic carbon layer (OPyC). The SiC layer is most important part of the containment system formed by the coating layers: it is the primary load bearer of internal pressure from fission gas and carbon monoxide potentially created by reaction of excess oxygen released from fission of uranium dioxide with the buffer, and it is the primary barrier to the release of fission products. Shrinkage of the dense PyC layers with increasing fast neutron fluence significantly reduces the tensile stress generated in the SiC layer during irradiation. Both PyC layers also act as retention barriers to fission gases. Finally, the buffer provides a void volume to accommodate fission gases and potential carbon monoxide, which helps reduce the deleterious pressure buildup. The buffer also attenuates fission-product recoil, which protects the IPyC layer, and it accommodates the swelling of the kernel during irradiation.

A multitude of phenomena have been historically observed in TRISO fuel particles undergoing irradiation, leading to the identification of failure mechanisms, i.e., failure of one or more coating layers. Models have been subsequently developed to accurately simulate these failure mechanisms with the intent of mitigating them by adequate fuel design (e.g., by optimizing particle geometry) or careful choice of irradiation conditions.

Modeling of these failure mechanisms relies on the knowledge of the material properties that underlie the behavior of the TRISO fuel particles under irradiation. These material properties have been primarily obtained from experimental data developed by historical TRISO fuel development programs in Europe and the United States. In some cases, incompleteness or uncertainty in some material properties requires that assumptions and approximations be made to establish a complete set of material properties for use in fuel performance modeling codes. Furthermore, some of these material properties were obtained from materials of different geometrical configurations (i.e., strip samples of flat geometry) and were assumed to be representative of coating layers with spherical geometry. The adequacy of these historical constitutive material properties is being evaluated as part of the Advanced Gas Reactor (AGR) Fuel Development and Qualification Program (INL, 2017). Our goal to identify the material properties that have the largest impact on the failure probability of TRISO-coated fuel particles under irradiation and to determine whether a need or requirement exists to re-evaluate any of these material property values for use in fuel-performance modeling codes.

2. FUEL IRRADIATION BEHAVIOR AND FAILURE MECHANISMS IN PARFUME

The PARticle FUel ModEl code (PARFUME) models the behavior of TRISO particles under irradiation. The irradiation effects are described using material, thermal, and physico-chemical properties, the relative importance of which are assessed in this report. The fuel kernel, buffer, and outer coating layers (both PyC and SiC) have specific properties that determine the fate of the TRISO particle under irradiation.

Coated-particle fuel exhibits statistical variations in physical dimensions and material properties from particle to particle due to the nature of its fabrication process. Many of the failure mechanisms are potentially multi-dimensional (3D), requiring more sophisticated fuel-particle analysis. PARFUME physically describes both the mechanical and physico-chemical behaviors of the fuel particle under irradiation while capturing the statistical variability of the fuel properties. From these behaviors, the code determines the possible failure of the fuel particle from established failure mechanisms.

Early during irradiation, shrinkage of the PyC layers puts the SiC layer in compression. The shrinkage/swelling response of PyC is highly anisotropic and depends on the irradiation temperature and degree of anisotropy of the PyC (characterized using the Bacon Anisotropy Factor or BAF). Due to this anisotropy in pyrocarbon shrinkage behavior, the shrinkage differs in the radial and tangential directions. Shrinkage of the IPyC and OPyC layers puts a compressive stress on the SiC layer.

As irradiation progresses, internal pressure generated by gaseous fission products released by the kernel increases and contributes a tensile component to the hoop stress in the SiC layer. However, the shrinkage of the PyC layers dominates, keeping the SiC layer in compression. This shrinkage puts the PyC layers into tension but irradiation-induced creep relieves that tensile stress and thereby reduces somewhat the compressive stress in the SiC layer. If the gas pressure load becomes large enough, the tangential stress in the SiC layer can become tensile, although modern TRISO particles are designed to ensure tensile stresses do not develop under irradiation. Failure of the particle would be expected if the stress in the SiC layer reaches a value that exceeds its fracture strength. While the IPyC and OPyC layers both shrink and creep during irradiation, the SiC response in PARFUME is essentially limited to elastic behavior. Consequently, failure of the SiC layer results in an instantaneous release of elastic energy. In PARFUME, this release of energy is deemed sufficient to cause simultaneous failure of the pyrocarbon layers.

Historically, the first failure mechanism of TRISO fuel was identified to be pressure vessel failure of the particle. Pressure vessel failure occurs when pressure from released fission gases builds up and becomes high enough for the tangential stress in the SiC layer to reach its fracture strength. Carbon monoxide (CO) produced by reaction of a net excess of oxygen with the carbonaceous buffer also contributes to pressure build-up. (The net excess of free oxygen originates from oxygen released during the fission process that is not consumed by the fission products.) Little CO production is expected in uranium oxycarbide (UCO) fuel, whereas it can be important in uranium dioxide (UO_2) fuel, especially at high burnup and temperature. In the case of pressure vessel failure, the particle has historically been analyzed solely in the radial dimension because of the symmetry in the tangential and azimuthal directions in the perfectly spherical geometry.

In addition to the one-dimensional behavior of a symmetrical spherical fuel particle, several other mechanisms have historically been identified that can potentially lead to particle failure. PARFUME also considers this multi-dimensional behavior, with associated potential failure mechanisms including (Miller et al., 2009):

- Cracking of the IPyC layer
- Partial debonding of the IPyC from the SiC layer

- Pressure-vessel failure of an aspherical particle

- Kernel/SiC interaction resulting from the amoeba effect.

IPyC cracking occurs when irradiation-induced shrinkage of the IPyC induces a tensile stress that exceeds the tensile strength in that layer. A radial crack then develops in the IPyC layer that creates a local tensile stress in the SiC layer, leading to possible particle failure.

Partial debonding of the IPyC from the SiC occurs when irradiation-induced shrinkage of the IPyC induces a radial tensile stress at the interface between the IPyC and SiC layers that exceeds the bond strength between the two layers.

Asphericity affects the probability of failure at high internal pressure. PARFUME incorporates the effects of asphericity for particles that have a flat facet but are otherwise spherical. Because of discontinuities in the faceted particle geometry, the faceted portion of that particle typically incurs higher stress than spherical or ellipsoidal portions from pressure generated by released fission gases or CO. If the pressure builds up high enough, the tensile stress in the faceted portion can exceed the fracture strength of the SiC and lead to particle failure. Effects of ellipsoidal asphericity are small by comparison and ellipsoidal particles are rarely if ever seen in fabrication, and therefore are not included in the code (Miller and Wadsworth, 1994).

Finally, kernel migration, also called the amoeba effect, occurs when the fuel kernel of a particle is pushed towards the SiC layer under the influence of a temperature gradient. Because of the difference in equilibrium of the reaction $CO+CO \rightarrow CO_2+C$ on the hot and cold side of the particle, solid-phase carbon is transported to the cold side of the TRISO particle. This causes an effective movement of the kernel towards the opposite (hot) side. Particle failure is assumed to occur when the kernel comes into contact with the SiC layer. This effect is prominent with UO_2 kernels and very small with UCO kernels because no CO production is expected in UCO kernels.

To model the multi-dimensional behavior associated with IPyC cracking, IPyC-SiC debonding, and asphericity, PARFUME uses results of the detailed finite-element analysis program Abaqus FEA (Abaqus, 2007) in conjunction with results from its own closed-form one-dimensional solution to make a statistical approximation of the stress levels in any particle (Miller et al., 2003). These combined results determine the multi-dimensional statistical parameters for cracking, debonding, and particle asphericity required as user inputs. The Abaqus model of a TRISO fuel particle consists of the three coating layers only; the kernel and buffer are not explicitly modeled. Their influence is considered through internal pressure calculated independently by PARFUME.

In PARFUME calculations, the buffer is assumed to stay bonded to the kernel and to completely detach from the IPyC layer as it densifies under irradiation, hence forming a so-called buffer-IPyC gap. The formation of this gap has two main consequences: first, it creates two independent mechanical systems, the kernel/buffer system and the system formed by the three outer coating layers; second, the gap provides a thermal insulating layer between these two systems because of its low thermal conductivity. The mechanical separation of the two systems dictates that the failure of the TRISO particle does not directly depend on the strain in the kernel or buffer caused by swelling and shrinkage, respectively. Furthermore, the temperature-dependent material properties of the coating layers are not affected by the kernel/buffer system because these layers are thermally insulated from it by the buffer-IPyC gap. Thus, the temperatures of the coating layers are determined by the boundary temperature of the matrix/coolant set at the outer surface of the OPyC layer. However, the kernel/buffer system has an indirect mechanical impact on the coating layers through fission gas pressure. Fission gas release from the kernel is a thermally driven process, calculated with a traditional Booth diffusion model (Booth, 1957); the fission gas pressure is determined by a pressure-volume-temperature equation of state for the fission gas. This representation of a fully detached buffer and IPyC layer stems from post-irradiation examination (PIE) data from historical irradiations. More extensive PIE conducted on AGR particles has revealed that

particles can also persist with a partially or fully intact buffer-IPyC interface at the end of irradiation, as observed by AGR-1 PIE (Demkowicz et al., 2016).

The width of the buffer-IPyC gap evolves during irradiation as the buffer and IPyC shrink with increasing neutron fast fluence while the kernel swells with increasing burnup. In a typical TRISO particle irradiation simulation, the gap stays open during irradiation, keeping both mechanical systems separate. PARFUME then calculates the failure probability of the TRISO particle by considering the stress developing in its coating layers. In its current form, PARFUME is not designed to deal with any mechanical interaction between the kernel/buffer system and the three outer coating layers. However, it has been predicted that mechanical interaction between the kernel/buffer system and the three outer coating layers would rapidly lead to the fracture of the SiC layer (Martin, 2002), although this has never been observed in TRISO fuel irradiations.

3. METHODOLOGY

The importance of TRISO fuel material properties is assessed by parametric variations of each property on the calculated stress in the particle layers and on the resultant failure probability of a TRISO-coated fuel particle under representative irradiation conditions. These irradiation conditions are detailed in Table 1. They correspond to average values for the AGR-5/6 irradiation which serves as the qualification experiment of the AGR TRISO fuel design. The temperatures of 700–1300°C were chosen to fall within the range of applicability of the material properties, which is typically 600–1350°C (Miller et al., 2009).

Table 1. Irradiation conditions.

Condition	EFPD	Burnup (%FIMA)	Fast fluence ($\times 10^{25}$ n/m^2, E > 0.18 MeV)	Irradiation Temperature (°C)
1	500	13.5	5	700
2	500	13.5	5	1000
3	500	13.5	5	1300

The failure probability of a TRISO particle under the irradiation conditions of Table 1 is calculated by PARFUME with the fuel parameters given in Table 2 and using the material properties described in the PARFUME Theory and Model Basis Report. The fuel parameters are based on the AGR-5/6/7 fuel specification (Marshall, 2017).

Table 2. Fuel parameters used in PARFUME modeling.

Category	Parameter	Nominal Value ± Standard Deviation
Fuel characteristics	^{235}U enrichment (wt%)	15.5
	Carbon/uranium (atomic ratio)	0.4
	Oxygen/uranium (atomic ratio)	1.5
	Uranium contamination fraction	0
Particle geometry	Kernel diameter (μm)	425 ± 10
	Buffer thickness (μm)	100 ± 10
	IPyC / OPyC thickness (μm)	40 ± 3
	SiC thickness (μm)	35 ± 2
	Particle asphericity (SiC aspect ratio)	1.040
Fuel properties	Kernel density (g/cm^3)	11.0
	Kernel theoretical density (g/cm^3)	11.4
	Buffer density (g/cm^3)	1.05
	Buffer theoretical density (g/cm^3)	2.25
	IPyC density (g/cm^3)	1.90 ± 0.02
	OPyC density (g/cm^3)	1.90 ± 0.02
	IPyC/OPyC (post compact anneal) BAF	1.05 ± 0.005

The material properties are varied around their nominal values by applying sensitivity multiplication factors (SMF) that bound both their anticipated values under the range of irradiation conditions of Table 1 and fuel properties of Table 2 and their potential uncertainty based on existing literature data. The failure probability is then computed again and the importance of the material properties to the failure probability

of the TRISO particle is assessed by comparing the failure probabilities for the nominal and sensitivity calculations.

Specific Abaqus FEA calculations were run for each SMF at all three irradiation temperatures to ensure the multi-dimensional coefficients used in PARFUME to calculate the SiC failure probability are consistent with the modified material properties. Because current U.S. TRISO fuel particle fabrication is originally based on the historic German fabrication processes, the IPyC-SiC bond strength is set at a value that is considered to be representative for German particles (50 MPa). At this bond strength, IPyC-SiC debonding is not predicted by PARFUME. As a consequence, debonding was not included in the calculation of the multi-dimensional input parameters. Similarly, the calculated internal pressure generated from UCO fuel in the irradiation conditions of this study is too low to lead to significant pressure-vessel failure of aspherical particles. Consequently, the importance of material properties to the asphericity failure mechanism was not considered.

4.   PARFUME CALCULATIONS

Using the input data from Table 1 and Table 2 and the baseline set of material properties in PARFUME, the failure probability of TRISO particles is computed by PARFUME for nominal conditions. Table 3 shows the resulting probabilities of SiC failure and IPyC cracking. These results serve as reference values to assess the impact of a variation of material properties on these failure probabilities. Similarly, Figure 1 shows the tangential stress at the inner surface of the SiC layer in the nominal conditions. This stress value is important as it is used to determine whether a particle fails. Fracture of SiC depends not only on the maximum stress in the layer, but also on stress distribution and volume under stress. Therefore, the values in Figure 1 are not, by themselves, sufficient to determine whether a particle fails. Weibull analysis based on the stress distribution over the volume of the SiC layer and the characteristic strength of the layer is used in PARFUME to determine the structural integrity of the particle. Furthermore, the stresses shown in Figure 1 apply to particles with the nominal fuel characteristics (nominal values in Table 2), i.e., they are not necessarily representative of the stresses for the particles in the tails of the distributions in Table 2, the characteristics of which are taken into account in the Weibull analysis and the subsequent results given in Table 3. In Figure 1, negative stress values indicate compressive stress, while positive values denote tensile stress. Excessive tensile stress is responsible for failure of the coating layers.

Table 3. Failure probability in the nominal conditions.

| Condition | Probability of SiC failure | | | Probability of IPyC cracking |
	Total	Contribution from IPyC Cracking	Contribution from Pressure	
1	4.03×10^{-4}	4.03×10^{-4}	0	8.94×10^{-1}
2	2.52×10^{-6}	2.52×10^{-6}	0	5.48×10^{-2}
3	2.21×10^{-9}	2.21×10^{-9}	2.82×10^{-13}	1.16×10^{-3}
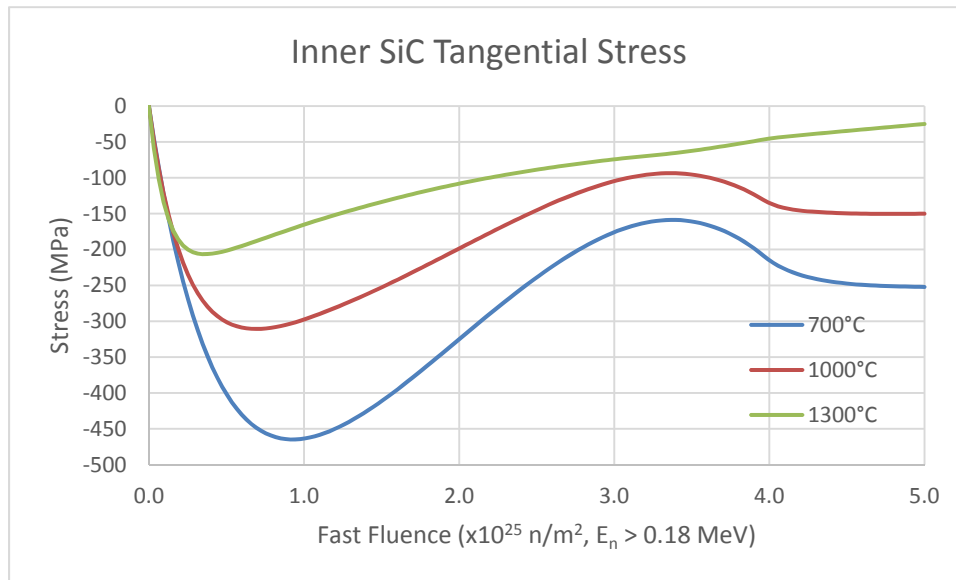
Figure 1. Tangential stress at the inner surface of the SiC layer in the nominal conditions.

Material properties are then varied by applying SMFs to their point values or functional relationships. The SMFs are chosen to bound the range of values found in the literature (and from which the values and functional relationships of the material properties are derived) and to extend beyond their boundaries for additional conservatism. It should be noted at these extreme boundary conditions, the values in question

can be unrealistic but are provided to give context to when the material property in question begins to impact particle failures even though in some cases, it is not physically possible.

For each material property, TRISO failure probability is re-calculated using the irradiation conditions in Table 1 for the various SMF and results compared to those given in Table 3.

5. MATERIAL PROPERTIES: KERNEL

5.1 Swelling

The kernel swelling rate (S) is given by:

$$\frac{S}{B_u} = \frac{\Delta V/V_0}{B_u} = 0.8\%/(\%FIMA)$$

where V_0 is the initial volume of the kernel and ΔV is the kernel volume increase during a time step at burnup B_u.

Kernel swelling occurs throughout irradiation as solid and gaseous fission products build up in the kernel. Experimental data suggest a strong correlation of kernel swelling to burnup. The kernel swelling rate used in PARFUME does not differentiate between solid and gaseous swelling, and it uses a single constant swelling rate that agrees with the UO_2 solid swelling rate recommended by MATPRO for LWRs (Siefken et al. 2001). Because burnups reached in LWRs are lower than in HTGRs, the validity of the swelling rate in PARFUME is limited to a range narrower than the range of burnup normally experienced by TRISO fuel.

Due to the lack of published data on UCO kernel swelling, PARFUME uses the same swelling rate for UCO and UO_2.

Review of literature

MATPRO reports solid-fission-product swelling rates ranging from 0.3 to 1.4%/(%FIMA) and it recommends a value of 0.76%/(%FIMA). It also mentions that data on LWR-fuel swelling indicate that gaseous swelling saturates at relatively low burnup. Post-irradiation examination on AGR-1 UCO TRISO fuel showed kernel swelling exceeding predictions and corresponding to a total swelling rate of about 1.6%/(%FIMA) (Bower et al. 2017). Kernel swelling in TRISO particles could be under predicted because modeling relies on fuel-swelling data obtained from LWR fuel pellets undergoing irradiation under different thermo-mechanical constraints than TRISO-coated fuel particles or because UO_2 and UCO fuel have inherently different behavior under irradiation.

Range of variation

Overall range of variation: 0.3–1.6%/(%FIMA)

PARFUME value: 0.8%/(%FIMA)

Sensitivity study

To account for this observed range in UO_2 swelling from MATPRO and the results on UCO fuel from the AGR-1 experiment, a sensitivity multiplication factor from 0.33 to 3 is applied to the kernel swelling rate in PARFUME. Table 4 shows the impact of kernel swelling on the failure probability of TRISO fuel under the irradiation conditions of Table 1. Results show that variations of the kernel-swelling rate have no impact on the probability of SiC failure. This is primarily due to the model assuming buffer-IPyC detachment.

Table 4. Failure probability: kernel swelling.

Condition	Sensitivity Multiplication Factor	Probability of SiC failure	Probability of IPyC cracking
1	0.33	4.03×10^{-4}	8.94×10^{-1}
	0.5	4.03×10^{-4}	8.94×10^{-1}
	1 (nominal)	4.03×10^{-4}	8.94×10^{-1}
	2	4.03×10^{-4}	8.94×10^{-1}
	3	4.03×10^{-4}	8.94×10^{-1}
2	0.33	2.52×10^{-6}	5.48×10^{-2}
	0.5	2.52×10^{-6}	5.48×10^{-2}
	1 (nominal)	2.52×10^{-6}	5.48×10^{-2}
	2	2.52×10^{-6}	5.48×10^{-2}
	3	2.52×10^{-6}	5.48×10^{-2}
3	0.33	2.21×10^{-9}	1.16×10^{-3}
	0.5	2.21×10^{-9}	1.16×10^{-3}
	1 (nominal)	2.21×10^{-9}	1.16×10^{-3}
	2	2.21×10^{-9}	1.16×10^{-3}
	3	2.21×10^{-9}	1.16×10^{-3}

5.2 Thermal Conductivity

The kernel thermal conductivity (k) is given by:

$$k(T) = 0.0132 \times e^{0.00188 \times T} + \frac{4040}{464+T} \quad \text{if } T < 1650°C$$

W/(m·K), T in °C

$$k(T) = 0.0132 \times e^{0.00188 \times T} + 1.9 \quad \text{if } T \geq 1650°C$$

The thermal conductivity of the kernel is a function of its temperature (Nabielek et al. 1992). In these PARFUME calculations, it varies from about 2.3 to 3.5 W/(m·K).

Review of literature

MATPRO reports thermal conductivity values in the range of 2.1 to 4.0 W/(m·K) for UO_2 fuel in the range of fuel temperatures of this study (Siefken et al., 2001), while the thermal conductivity of the UO_2 kernel in Commissariat à l'énergie atomique et aux énergies alternatives (CEA) fuel-performance modeling code can vary from 1.9 to 3.5 W/(m·K) (I-NERI, 2004). Additionally, Harding and Martin (1989) and Ronchi et al. (1999) suggest values from 2.6 to 4.0 W/(m·K) and 2.3 to 3.3 W/(m·K), respectively, in the same temperature range.

Due to the lack of published data on UCO thermal conductivity, PARFUME uses UO_2 data for UCO kernels.

Range of variation

Overall range of variation: 1.9–4.0 W/(m·K)

PARFUME range: 2.3–3.5 W/(m·K)

Sensitivity study

Applying SMF to the thermal conductivity of the kernel in PARFUME, Table 5 shows its impact on the failure probability of TRISO fuel under the irradiation conditions of Table 1. Results show that variations of the kernel thermal conductivity have no impact on the probability of SiC failure.

Table 5. Failure probability: kernel thermal conductivity.

Condition	Sensitivity Multiplication Factor	Probability of SiC failure	Probability of IPyC cracking
1	0.33	4.03×10^{-4}	8.94×10^{-1}
	0.5	4.03×10^{-4}	8.94×10^{-1}
	1 (nominal)	4.03×10^{-4}	8.94×10^{-1}
	2	4.03×10^{-4}	8.94×10^{-1}
	3	4.03×10^{-4}	8.94×10^{-1}
2	0.33	2.52×10^{-6}	5.48×10^{-2}
	0.5	2.52×10^{-6}	5.48×10^{-2}
	1 (nominal)	2.52×10^{-6}	5.48×10^{-2}
	2	2.52×10^{-6}	5.48×10^{-2}
	3	2.52×10^{-6}	5.48×10^{-2}
3	0.33	2.21×10^{-9}	1.16×10^{-3}
	0.5	2.21×10^{-9}	1.16×10^{-3}
	1 (nominal)	2.21×10^{-9}	1.16×10^{-3}
	2	2.21×10^{-9}	1.16×10^{-3}
	3	2.21×10^{-9}	1.16×10^{-3}

5.3   Summary of the Material Properties of the Kernel

The material properties of the kernel used in PARFUME are:

- Swelling rate

- Thermal conductivity

There is significant uncertainty in the kernel swelling rate because the historical values based on low burnup UO_2 are not accurately matched by the results of the AGR-1 PIE data based on higher burnup UCO. Because the buffer is assumed detached from the IPyC, the swelling of the kernel has no impact on the integrity of the coating layers. Similarly, the uncertainty on the thermal conductivity of the kernel does not affect the probability of failure of the coating layers, although it is used to calculate the temperature in the kernel that determines the pressure of the fission gases.

6. MATERIAL PROPERTIES: BUFFER

6.1 Elastic Modulus

The elastic modulus of the buffer (E) is given by:

$$E = 25.5 \times (0.384 + 0.324 \times \rho) \times (1 + 0.23 \times \Phi) \times \left(1 + 1.5 \times 10^{-4} \times (T - 20)\right) \text{GPa, T in °C}$$

The expression given here for the elastic modulus of the buffer is the functional relationship used in the source code of PARFUME.

The elastic modulus of the buffer varies with density, fast fluence, and temperature. In these calculations, it varies from 21 to 50 GPa.

Review of literature

British Nuclear Fuels, Ltd. (BNFL) fuel-performance modeling codes use their own functional relationship with resulting variations of the elastic modulus from 13 to 25 GPa, while Forschungszentrum Jülich (FZJ) models use an elastic modulus of 10 GPa (I-NERI, 2004). The CEGA report recommends a fixed value of 11 GPa (CEGA, 1993).

Range of variation

Overall range of variation: 10–50 GPa

PARFUME range: 21–50 GPa

Sensitivity study

Applying SMF to the elastic modulus of the buffer in PARFUME, Table 6 shows its impact on the failure probability of TRISO fuel under the irradiation conditions of Table 1. Results show that variations of the buffer elastic modulus have no impact on the probability of SiC failure.

Table 6. Failure probability: buffer elastic modulus.

Condition	Sensitivity Multiplication Factor	Probability of SiC failure	Probability of IPyC cracking
1	0.2	4.03×10^{-4}	8.94×10^{-1}
	0.5	4.03×10^{-4}	8.94×10^{-1}
	1 (nominal)	4.03×10^{-4}	8.94×10^{-1}
	2	4.03×10^{-4}	8.94×10^{-1}
	5	4.03×10^{-4}	8.94×10^{-1}
2	0.2	2.52×10^{-6}	5.48×10^{-2}
	0.5	2.52×10^{-6}	5.48×10^{-2}
	1 (nominal)	2.52×10^{-6}	5.48×10^{-2}
	2	2.52×10^{-6}	5.48×10^{-2}
	5	2.52×10^{-6}	5.48×10^{-2}
3	0.2	2.21×10^{-9}	1.16×10^{-3}
	0.5	2.21×10^{-9}	1.16×10^{-3}
	1 (nominal)	2.21×10^{-9}	1.16×10^{-3}
	2	2.21×10^{-9}	1.16×10^{-3}
	5	2.21×10^{-9}	1.16×10^{-3}

6.2   Poisson's Ratio

The Poisson's ratio of the buffer (μ) is given by:

$\mu = 0.33$

The expression given here for the Poisson's ratio of the buffer is the value used in the source code of PARFUME.

The dependency of the Poisson's ratio on density, fast fluence, and temperature is largely unknown. Therefore, the Poisson's ratio is assumed independent of these parameters and kept constant throughout irradiation.

Review of literature

Values of 0.21 and 0.3 have been recommended by the BNFL and FZJ models, respectively (I-NERI, 2004). Additionally, by definition and assuming expansion in the transverse direction under compression in the longitudinal one, the Poisson's ratio ranges from 0 to 0.5.

Range of variation

Overall range of variation: 0–0.5

PARFUME value: 0.33

Sensitivity study

Assuming values of the Poisson's ratio of the buffer between 0 and 0.5, Table 7 shows its impact on the failure probability of TRISO fuel under the irradiation conditions of Table 1. Results show that variations of the buffer Poisson's ratio have no impact on the probability of SiC failure.

Table 7. Failure probability: buffer Poisson's ratio.

Condition	Poisson's ratio	Probability of SiC failure	Probability of IPyC cracking
1	0	4.03×10^{-4}	8.94×10^{-1}
	0.25	4.03×10^{-4}	8.94×10^{-1}
	0.33 (nominal)	4.03×10^{-4}	8.94×10^{-1}
	0.4	4.03×10^{-4}	8.94×10^{-1}
	0.5	4.03×10^{-4}	8.94×10^{-1}
2	0	2.52×10^{-6}	5.48×10^{-2}
	0.25	2.52×10^{-6}	5.48×10^{-2}
	0.33 (nominal)	2.52×10^{-6}	5.48×10^{-2}
	0.4	2.52×10^{-6}	5.48×10^{-2}
	0.5	2.52×10^{-6}	5.48×10^{-2}
3	0	2.21×10^{-9}	1.16×10^{-3}
	0.25	2.21×10^{-9}	1.16×10^{-3}
	0.33 (nominal)	2.21×10^{-9}	1.16×10^{-3}
	0.4	2.21×10^{-9}	1.16×10^{-3}
	0.5	2.21×10^{-9}	1.16×10^{-3}

6.3   Irradiation-induced Creep

Irradiation-induced creep of the buffer (K_S) is given by:

$$K_S = C_{amp} \times [1 + 2.38 \times (1.9 - \rho)]$$
$$\times (2.193 \times 10^{-4} - 4.85 \times 10^{-7} \times T + 4.0147 \times 10^{-10} \times T^2) \qquad \times 10^{-25} \ (\text{MPa-n/m}^2)^{-1}, \ T \text{ in } °C$$

Due to the absence of data for porous carbon, the correlation for PyC is used (see Section 7.3) and adjusted to the lower density of the buffer. Transient state creep is not explicitly detailed in PARFUME but a "creep amplification" coefficient, C_{amp}, is used to vary the amplitude of the irradiation-induced creep to account for uncertainty in its value. In these calculations and using a $C_{amp} = 2$ (based on benchmark data), the irradiation-induced creep coefficient of the buffer varies from about 3.7 to $16.6 \times 10^{-29} \ (\text{MPa-n/m}^2)^{-1}$. This range can be reduced or amplified by adjusting the coefficient C_{amp}.

Review of literature

The functional relationship for irradiation-induced creep of the buffer is the same used for the PyC layers. A review of existing data is discussed in the PyC section of this report. Additionally, FZJ and BNFL fuel-performance modeling codes use irradiation-induced creep values of 1.1 and $4.8 \times 10^{-29} \ (\text{MPa-n/m}^2)^{-1}$, respectively (I-NERI,2004).

Range of variation

Overall range of variation: $1.1–16.6 \times 10^{-29} (\text{MPa-n/m}^2)^{-1}$

PARFUME range: $3.7–16.6 \times 10^{-29} (\text{MPa-n/m}^2)^{-1}$

Sensitivity study

Applying SMF to the irradiation-induced creep in the buffer, Table 8 shows its impact on the failure probability of TRISO fuel under the irradiation conditions of Table 1. Results show that variations of the buffer irradiation-induced creep have no impact on the probability of SiC failure.

Table 8. Failure probability: buffer irradiation-induced creep.

Condition	Sensitivity Multiplication Factor	Probability of SiC failure	Probability of IPyC cracking
1	0.05	4.03×10^{-4}	8.94×10^{-1}
	0.2	4.03×10^{-4}	8.94×10^{-1}
	1 (nominal)	4.03×10^{-4}	8.94×10^{-1}
	5	4.03×10^{-4}	8.94×10^{-1}
	20	4.03×10^{-4}	8.94×10^{-1}
2	0.05	2.52×10^{-6}	5.48×10^{-2}
	0.2	2.52×10^{-6}	5.48×10^{-2}
	1 (nominal)	2.52×10^{-6}	5.48×10^{-2}
	5	2.52×10^{-6}	5.48×10^{-2}
	20	2.52×10^{-6}	5.48×10^{-2}
3	0.05	2.21×10^{-9}	1.16×10^{-3}
	0.2	2.21×10^{-9}	1.16×10^{-3}
	1 (nominal)	2.21×10^{-9}	1.16×10^{-3}
	5	2.21×10^{-9}	1.16×10^{-3}
	20	2.21×10^{-9}	1.16×10^{-3}

6.4 Poisson's Ratio in Creep

Poisson's ratio in creep of the buffer (ν) is given by:

$$\nu = 0.5$$

It is assumed constant during irradiation.

Review of literature

The value for the Poisson's ratio in creep of the buffer is the same used for the PyC layers. A review of existing data is discussed in the PyC section of this report. Additionally, the FZJ and BNFL models use values of 0.5 and 0.4, respectively (I-NERI, 2004).

Range of variation

Overall range of variation: 0–0.5

PARFUME value: 0.5

Sensitivity study

Assuming values of the Poisson's ratio in creep between 0 and 0.5, Table 9 shows its impact on the failure probability of TRISO fuel under the irradiation conditions of Table 1. Results show that variations of the buffer Poisson's ratio in creep have no impact on the probability of SiC failure.

Table 9. Failure probability: buffer Poisson's ratio in creep.

Condition	Poisson's ratio	Probability of SiC failure	Probability of IPyC cracking
1	0	4.03×10^{-4}	8.94×10^{-1}
	0.25	4.03×10^{-4}	8.94×10^{-1}
	0.4	4.03×10^{-4}	8.94×10^{-1}
	0.5 (nominal)	4.03×10^{-4}	8.94×10^{-1}
2	0	2.52×10^{-6}	5.48×10^{-2}
	0.25	2.52×10^{-6}	5.48×10^{-2}
	0.4	2.52×10^{-6}	5.48×10^{-2}
	0.5 (nominal)	2.52×10^{-6}	5.48×10^{-2}
3	0	2.21×10^{-9}	1.16×10^{-3}
	0.25	2.21×10^{-9}	1.16×10^{-3}
	0.4	2.21×10^{-9}	1.16×10^{-3}
	0.5 (nominal)	2.21×10^{-9}	1.16×10^{-3}

6.5 Irradiation-induced Dimensional Change and Strain Rate

The irradiation-induced strain rate of the buffer ($\dot{\varepsilon}$) is given by:

$$\dot{\varepsilon} = \frac{d\varepsilon}{d\Phi} = b_0 + b_1 \times \Phi + b_2 \times \Phi^2 + b_3 \times \Phi^3 \qquad \times (10^{25} \text{n/m}^2)^{-1}$$

where the b_i coefficients depend on density and temperature. The buffer strain (also known as dimensional change) is obtained by integrating its strain rate over fast fluence; the resulting coefficients are detailed in the CEGA report and in the *PARFUME Theory and Model Basis Report*. The variations of the buffer strain rate and buffer strain with fast fluence for a buffer density of 1.05 g/cm^3 at two extremum temperatures are shown in Figure 2. The buffer stain rate has a cut-off in fast fluence at 4×10^{25} n/m^2 and

it remains equal to its value at the cut-off for higher fast fluences. In these calculations, the buffer strain rate varies between -0.081 and -0.009 $\times (10^{25} \text{n/m}^2)^{-1}$.

Review of literature

Figure 2 also shows the correlations used in the FZJ and BNFL fuel performance modeling codes (I-NERI, 2004). The corresponding strain rates only vary with fluence. For fast fluences between 0 and 5×10^{25} n/m^2, they vary from -0.193 to ~$10^{-5}\times(10^{25}\text{n/m}^2)^{-1}$ and -0.265 to ~$10^{-6}\times(10^{25}\text{n/m}^2)^{-1}$, respectively.

Range of variation

Overall range of variation: $-0.265 - \sim 10^{-6} \times (10^{25}\text{n/m}^2)^{-1}$

PARFUME value: $-0.081 - -0.009 \times (10^{25}\text{n/m}^2)^{-1}$
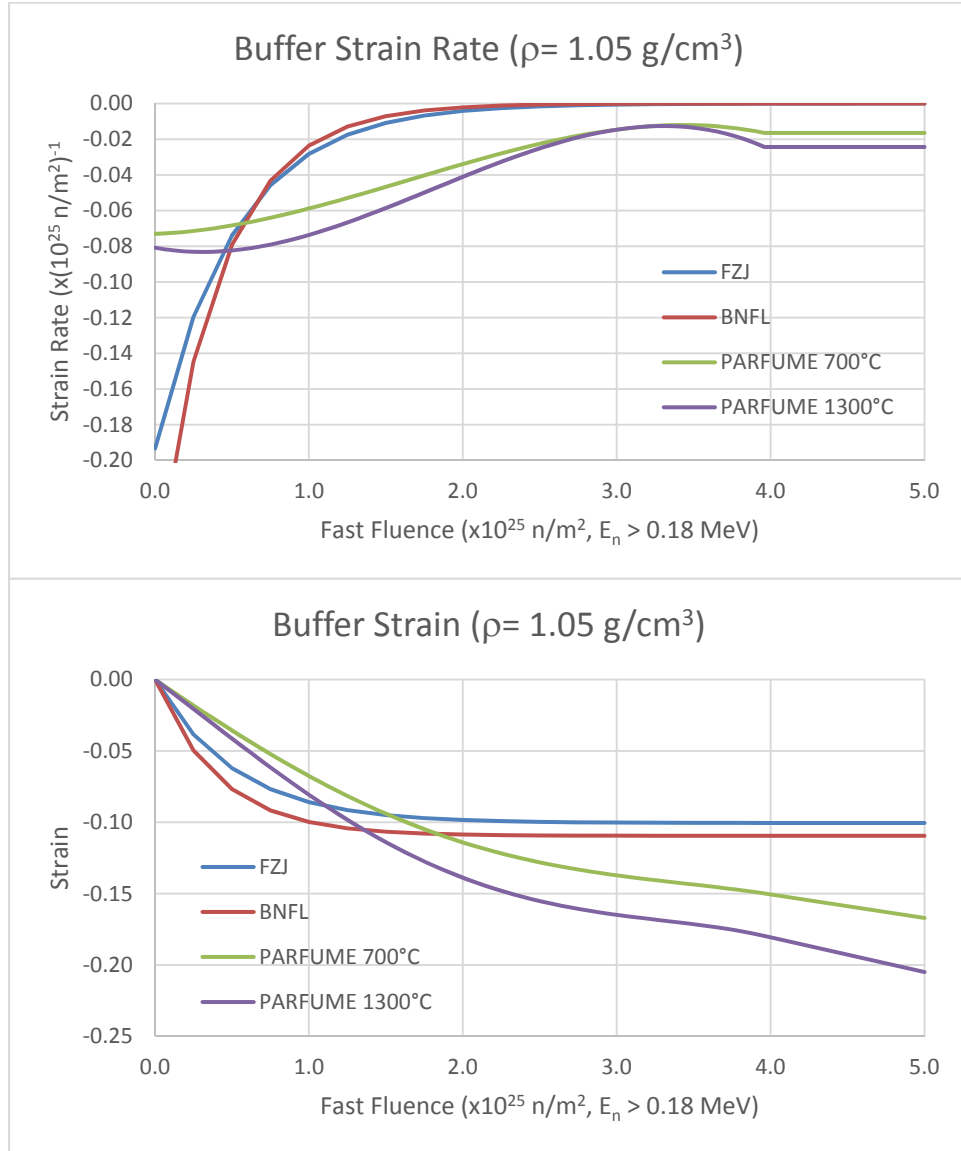
Figure 2. Buffer strain rate (top) and buffer strain (bottom) used in PARFUME along with BNFL and FZJ correlations. A negative strain denotes shrinkage.

Sensitivity study

Applying SMF that cover the range of variation of the buffer strain rate, Table 10 shows the impact of the irradiation-induced dimensional change in the buffer on the failure probability of TRISO fuel under the irradiation conditions of Table 1. Results show that variations of the buffer strain rate have no impact on the probability of SiC failure.

Table 10. Failure probability: buffer irradiation-induced dimensional change.

Condition	Sensitivity Multiplication Factor	Probability of SiC failure	Probability of IPyC cracking
	0.1	4.03×10^{-4}	8.94×10^{-1}
	0.33	4.03×10^{-4}	8.94×10^{-1}
	1 (nominal)	4.03×10^{-4}	8.94×10^{-1}
1	3	4.03×10^{-4}	8.94×10^{-1}
	10	4.04×10^{-4}	8.94×10^{-1}
	BNFL	4.04×10^{-4}	8.94×10^{-1}
	FZJ	4.03×10^{-4}	8.94×10^{-1}
	0.1	2.52×10^{-6}	5.48×10^{-2}
	0.33	2.52×10^{-6}	5.48×10^{-2}
	1 (nominal)	2.52×10^{-6}	5.48×10^{-2}
2	3	2.52×10^{-6}	5.48×10^{-2}
	10	2.51×10^{-6}	5.47×10^{-2}
	BNFL	2.52×10^{-6}	5.48×10^{-2}
	FZJ	2.52×10^{-6}	5.47×10^{-2}
	0.1	2.21×10^{-9}	1.16×10^{-3}
	0.33	2.21×10^{-9}	1.16×10^{-3}
	1 (nominal)	2.21×10^{-9}	1.16×10^{-3}
3	3	2.21×10^{-9}	1.16×10^{-3}
	10	2.28×10^{-9}	1.16×10^{-3}
	BNFL	2.20×10^{-9}	1.16×10^{-3}
	FZJ	2.21×10^{-9}	1.16×10^{-3}

6.6   Thermal Conductivity

Thermal conductivity of the buffer (k) is given by:

$$k = \frac{k_0 \times k_{th} \times \rho_{th} \times (\rho_{th} - \rho_0)}{k_{th} \times \rho_{th} \times (\rho_{th} - \rho) + k_0 \times \rho \times (\rho - \rho_0)} \qquad W/(m \cdot K)$$

Thermal conductivity of the buffer depends on its actual density ($\rho_0 = \sim 1$ g/cm^3) and theoretical density ($\rho_{th} = 2.25$ g/cm^3) and on the thermal conductivities at these two densities ($k_0 = 0.5$ W/[m·K] and $k_{th} = 4$ W/[m·K]). It is assumed that the low density (~55% porosity) unirradiated buffer has an initial thermal conductivity of 0.5 W/(m·K) and that this conductivity increases as the buffer densifies throughout irradiation. The thermal conductivity of the buffer at its theoretical density (zero porosity) is assumed to be 4 W/(m·K). Hence, the thermal conductivity of the buffer can theoretically vary from 0.5 to 4 W/(m·K) but, in these calculations, it varies from 0.5 to 0.7 W/(m·K) as densification stays limited.

Review of literature

In BNFL TRISO fuel modeling, the thermal conductivity of the buffer increases with density and ranges from 2.5 to 4.0 W/(m·K) in these calculations while FZJ fuel performance modeling codes assume a constant value of 0.5 W/(m·K) (I-NERI, 2004). Similar values were obtained by Rochais et al. (2008), with conductivities of 0.4 and 0.64 W/(m·K) in the radial and circumferential directions, respectively. Salgado et al. (1971) report a value of 1.6 W/(m·K) while Lopez-Honorato et al. (2008b) measured a higher conductivity of 5.7 W/(m·K) at a density of 1.35 g/cm^3.

Range of variation

Overall range of variation: 0.4–5.7 W/(m·K)

PARFUME range: 0.5–0.7 W/(m·K)

Sensitivity study

Applying SMFs to the thermal conductivity of the buffer in PARFUME, Table 11 shows the impact of buffer thermal conductivity on the failure probability of TRISO fuel under the irradiation conditions of Table 1. Results show that variations of the buffer thermal conductivity have negligible impact on the probability of SiC failure. A lower buffer conductivity leads to a higher kernel temperature which enhances fission-gas release and internal pressure. The increased internal pressure counteracts somewhat the tensile shrinkage in the IPyC layer, which reduces its probability of cracking and subsequently decreases its contribution to the probability of SiC failure. Conversely, the higher internal pressure increases the probability of SiC failure by pressure-vessel failure. The overall impact on SiC failure probability results from the balance between these two phenomena and is more pronounced at higher irradiation temperatures.

Table 11. Failure probability: buffer thermal conductivity.

Condition	Sensitivity Multiplication Factor	Probability of SiC failure	Probability of IPyC cracking
1	0.1	4.03×10^{-4}	8.93×10^{-1}
	0.33	4.04×10^{-4}	8.94×10^{-1}
	1 (nominal)	4.03×10^{-4}	8.94×10^{-1}
	3	4.03×10^{-4}	8.94×10^{-1}
	10	4.03×10^{-4}	8.94×10^{-1}
2	0.1	2.50×10^{-6}	5.43×10^{-2}
	0.33	2.52×10^{-6}	5.47×10^{-2}
	1 (nominal)	2.52×10^{-6}	5.48×10^{-2}
	3	2.52×10^{-6}	5.48×10^{-2}
	10	2.52×10^{-6}	5.48×10^{-2}
3	0.1	2.91×10^{-9}	1.13×10^{-3}
	0.33	2.20×10^{-9}	1.16×10^{-3}
	1 (nominal)	2.21×10^{-9}	1.16×10^{-3}
	3	2.21×10^{-9}	1.17×10^{-3}
	10	2.21×10^{-9}	1.17×10^{-3}

6.7   Thermal Expansion

The thermal expansion coefficient of the buffer (α) is given by:

$$\alpha = 5 \times \left(1 + 0.11 \times \frac{T-400}{700}\right) \qquad \times 10^{-6}/°C, \text{ T in } °C$$

The coefficient of thermal expansion of the buffer is a function of temperature. In these calculations, it varies from about 5.2 to $5.8 \times 10^{-6}/°C$.

Review of literature

FZJ and BNFL fuel performance modeling codes use a slightly lower value of $3.5 \times 10^{-6}/K$ (I-NERI, 2004).

Range of variation

Overall range of variation: 3.5–$5.8 \times 10^{-6}/°C$

PARFUME value: 5.2–$5.8 \times 10^{-6}/°C$

Sensitivity study

Applying SMFs to the thermal expansion of the buffer in PARFUME, Table 12 shows the impact of buffer thermal expansion on the failure probability of TRISO fuel under the irradiation conditions of Table 1. Results show that variations of the buffer thermal expansion have no impact on the probability of SiC failure.

Table 12. Failure probability: buffer thermal expansion.

Condition	Sensitivity Multiplication Factor	Probability of SiC failure	Probability of IPyC cracking
1	0.5	4.03×10^{-4}	8.94×10^{-1}
	0.66	4.03×10^{-4}	8.94×10^{-1}
	1 (nominal)	4.03×10^{-4}	8.94×10^{-1}
	1.5	4.03×10^{-4}	8.94×10^{-1}
	2	4.03×10^{-4}	8.94×10^{-1}
2	0.5	2.52×10^{-6}	5.48×10^{-2}
	0.66	2.52×10^{-6}	5.48×10^{-2}
	1 (nominal)	2.52×10^{-6}	5.48×10^{-2}
	1.5	2.52×10^{-6}	5.48×10^{-2}
	2	2.52×10^{-6}	5.48×10^{-2}
3	0.5	2.21×10^{-9}	1.16×10^{-3}
	0.66	2.21×10^{-9}	1.16×10^{-3}
	1 (nominal)	2.21×10^{-9}	1.16×10^{-3}
	1.5	2.21×10^{-9}	1.16×10^{-3}
	2	2.21×10^{-9}	1.16×10^{-3}

6.8   Summary of the Material Properties of the Buffer

The material properties of the buffer used in PARFUME are

- Elastic modulus

- Poisson's ratio

- Irradiation-induced creep

- Poisson's ratio in creep

- Strain rates

- Thermal conductivity

- Thermal expansion.

Some of the material properties of the buffer (elastic modulus, irradiation-induced creep, strain rates, and thermal conductivity) exhibit large variabilities but the assumption of a fully debonded buffer ensures that the uncertainties on these properties do not affect the mechanical integrity of the IPyC and SiC layers.

7. MATERIAL PROPERTIES: PyC

7.1 Elastic Moduli

The elastic moduli of the PyC in the tangential (E_t) and radial (E_r) directions are given by:

$$E_t = 25.5 \times (0.384 + 0.324 \times \rho) \times (0.481 + 0.519 \times BAF)$$
$$\times (1 + 0.23 \times \Phi) \times \left(1 + 1.5 \times 10^{-4} \times (T - 20)\right) \qquad \text{GPa, T in °C}$$

$$E_r = 25.5 \times (0.384 + 0.324 \times \rho) \times (1.463 - 0.463 \times BAF)$$
$$\times (1 + 0.23 \times \Phi) \times \left(1 + 1.5 \times 10^{-4} \times (T - 20)\right) \qquad \text{GPa, T in °C}$$

The expressions given here for the radial and tangential elastic moduli of the PyC layers are the functional relationships used in the source code of PARFUME. They correspond to the functional relationships reported in the *PARFUME Theory and Model Basis Report* using a crystallite diameter size of 45 Å.

The elastic moduli of the PyC layers vary with density, BAF, fast fluence, and temperature. In these calculations, they vary from about 26 to 62 GPa.

Review of literature

BNFL fuel-performance modeling codes use a fluence-dependent PyC elastic modulus that spans from 25 to 50 GPa over the range of fast fluence in Table 1, while FZJ models use a constant value of 29 GPa (I-NERI, 2004). Kaae (1971) reports a density-dependent elastic modulus that ranges from 23 to 27 GPa with the parameters used in these calculations. Furthermore, Kaae et al. (1977) showed that the coating rate could also impact the elastic modulus, but only as a consequence of modifying other PyC characteristics such as density or BAF. Hosemann et al. (2013) cite PyC elastic modulus values between 20 to 30 GPa, in agreement with values 19 to 34 GPa reported by Lopez-Honorato et al. (2008a) for various coating conditions (deposition temperature and concentration of the precursor gases). Lopez-Honorato et al. (2008a) also showed how variations in these coating conditions affected the density of the PyC. Finally, Hofmann et al. (2000) and Bellan and Dhers (2014) report values of 24 and 26 GPa, respectively.

Range of variation

Overall range of variation: 19–62 GPa

PARFUME range: 26–62 GPa

Sensitivity study

Applying SMFs to the elastic moduli of the PyC layers in PARFUME, Table 13 shows their impact on the failure probability of TRISO fuel under the irradiation conditions of Table 1. Figure 3 shows the tangential stress at the inner surface of the SiC layer for the nominal PyC elastic moduli and SMF 0.33 and 3.

Figure 3 shows that an increase of the radial and tangential elastic moduli of the PyC leads to an increase of the compressive tangential stress in the SiC layer. As seen in Table 13, this also translates into an increase of the probabilities of IPyC cracking and SiC failure. These trends can be seen in Figure 4 that plots the results of Table 13.

To get a better appreciation of the impact of PyC elastic moduli on the probabilities of IPyC cracking and SiC failure, Figure 5 shows the relative difference between the probabilities of Table 13 and the nominal probabilities of Table 3. It shows that the probability of SiC failure can almost triple when the elastic moduli of the PyC are multiplied by a factor 3, however some of these values at extremes of the range are well beyond historically measured values.

Table 13. Failure probability: PyC elastic moduli.

Condition	Sensitivity Multiplication Factor	Probability of SiC failure	Probability of IPyC cracking
1	0.33	2.54×10^{-5}	1.38×10^{-1}
	0.5	1.15×10^{-4}	4.06×10^{-1}
	1 (nominal)	4.03×10^{-4}	8.94×10^{-1}
	2	5.92×10^{-4}	9.94×10^{-1}
	3	6.54×10^{-4}	9.99×10^{-1}
2	0.33	2.02×10^{-7}	9.04×10^{-3}
	0.5	6.62×10^{-7}	2.11×10^{-2}
	1 (nominal)	2.52×10^{-6}	5.48×10^{-2}
	2	5.29×10^{-6}	9.36×10^{-2}
	3	6.84×10^{-6}	1.14×10^{-1}
3	0.33	4.19×10^{-10}	2.72×10^{-4}
	0.5	9.24×10^{-10}	5.31×10^{-4}
	1 (nominal)	2.21×10^{-9}	1.16×10^{-3}
	2	3.69×10^{-9}	1.90×10^{-3}
	3	4.47×10^{-9}	2.29×10^{-3}
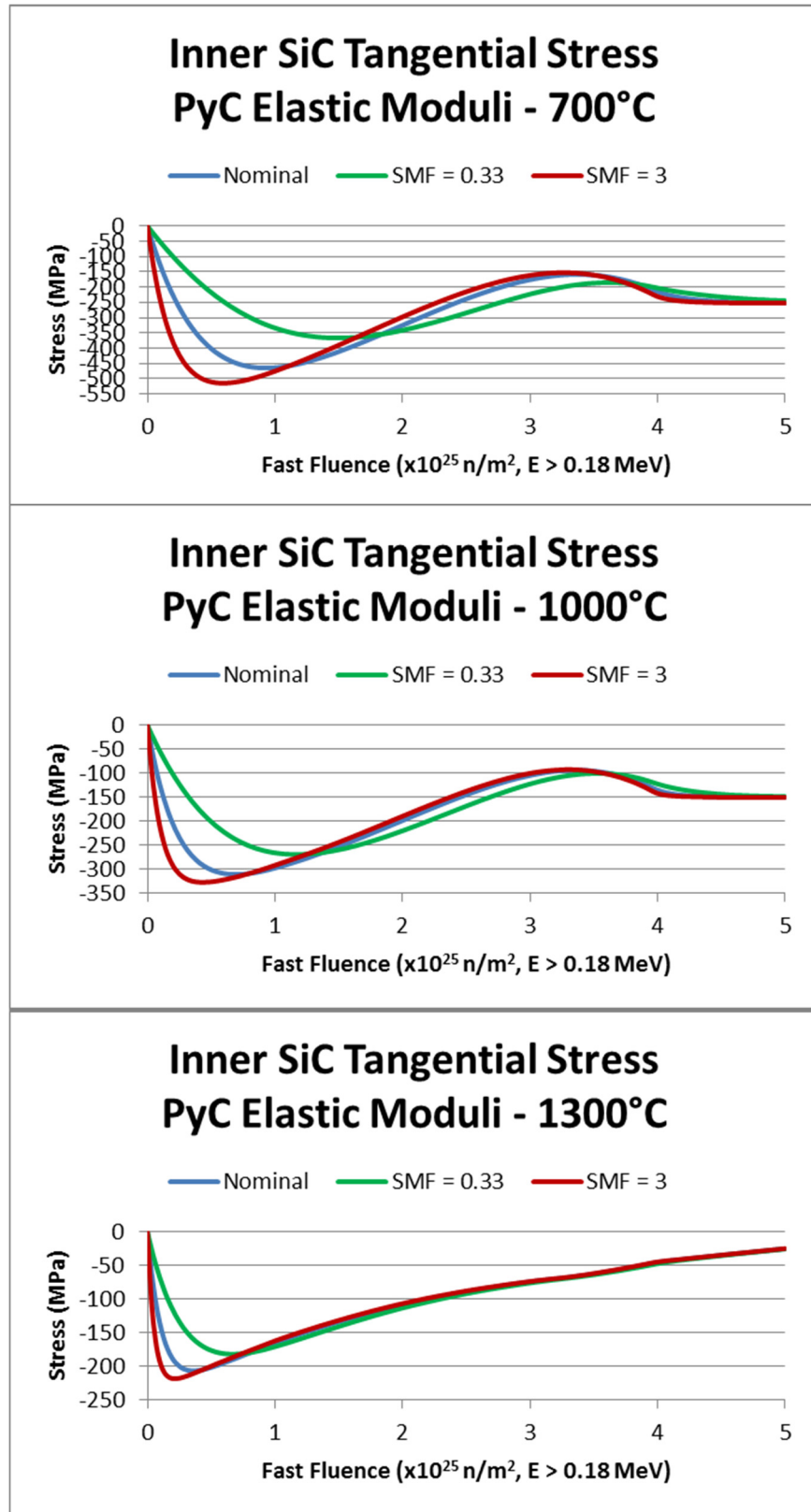
Figure 3. Tangential stress at the inner surface of the SiC layer for the nominal PyC elastic moduli and SMF 0.33 and 3.
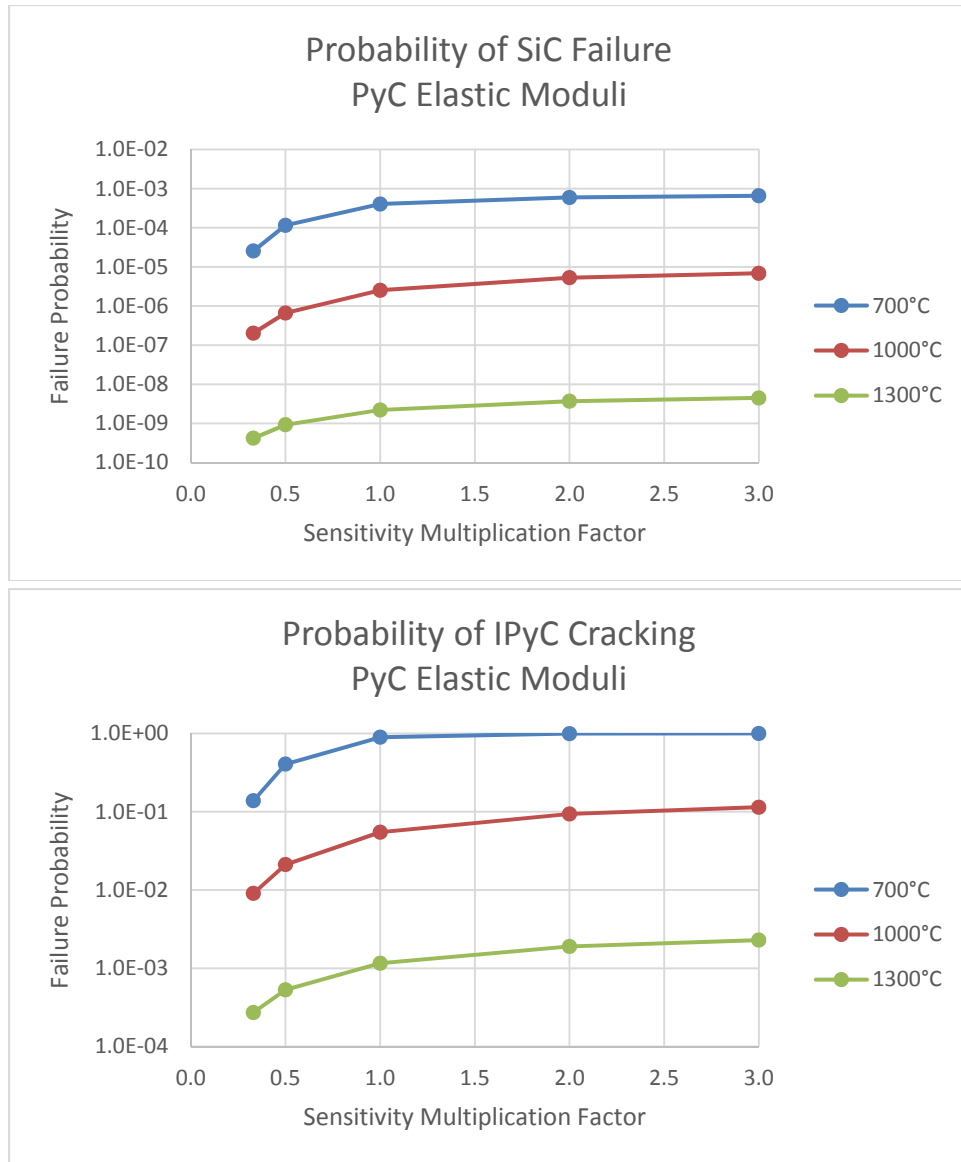
Figure 4. Probability of SiC failure (top) and IPyC cracking (bottom) as a function of the sensitivity multiplication factor applied to the PyC elastic moduli.

Figure 5. Ratio between the probability of SiC failure (top) and IPyC cracking (bottom) values and their nominal values as a function of the sensitivity multiplication factor applied to the PyC elastic moduli.

7.2   Poisson's Ratio

The Poisson's ratio of the PyC (μ) is given by:

μ = 0.33

The expression given here for the Poisson's ratio of the PyC is the value used in the source code of PARFUME.

The dependency of the PyC Poisson's ratio on density, BAF, fast fluence, and temperature is largely unknown. Therefore, the Poisson's ratio is assumed independent of these parameters and kept at a constant value of 0.33 throughout irradiation.

Review of literature

The CEGA report recommends a value for the PyC Poisson's ratio of 0.23. Price and Kaae (1969) suggested values of 0.21 and 0.24. Additionally, by definition and assuming expansion in the transverse direction under compression in the longitudinal one, the Poisson's ratio ranges from 0 to 0.5.

Range of variation

Overall range of variation: 0 to 0.5

PARFUME value: 0.33

Sensitivity study

Assuming values of the Poisson's ratio between 0 and 0.5, Table 14 shows its impact on the failure probability of TRISO fuel under the irradiation conditions of Table 1. Figure 6 shows the tangential stress at the inner surface of the SiC layer for the nominal PyC Poisson's ratio and extremum values 0 and 0.5.

Combined, Figure 6 and Table 14 show that an increase of the PyC Poisson's ratio also increases the compressive stress in the SiC layer and the probabilities of IPyC cracking and SiC failure. These trends can be seen in Figure 7 that plots the results of Table 14. Figure 8 shows the relative difference between the probabilities of Table 14 and the nominal probabilities of Table 3. It shows that the probability of SiC failure can increase by up to 60% when the PyC Poisson's ratio is increased to its maximum value of 0.5.

Table 14. Failure probability: PyC Poisson's ratio.

| Condition	Poisson's ratio	Probability of SiC failure	Probability of IPyC cracking
1	0	1.90×10^{-4}	5.60×10^{-1}
	0.25	3.50×10^{-4}	8.25×10^{-1}
	0.33 (nominal)	4.03×10^{-4}	8.94×10^{-1}
	0.4	4.48×10^{-4}	9.40×10^{-1}
	0.5	5.04×10^{-4}	9.79×10^{-1}
2	0	1.05×10^{-6}	2.86×10^{-2}
	0.25	2.03×10^{-6}	4.65×10^{-2}
	0.33 (nominal)	2.52×10^{-6}	5.48×10^{-2}
	0.4	3.04×10^{-6}	6.34×10^{-2}
	0.5	3.96×10^{-6}	7.80×10^{-2}
3	0	1.26×10^{-9}	6.86×10^{-4}
	0.25	1.91×10^{-9}	1.02×10^{-3}
	0.33 (nominal)	2.21×10^{-9}	1.16×10^{-3}
	0.4	2.50×10^{-9}	1.32×10^{-3}
	0.5	3.03×10^{-9}	1.59×10^{-3}
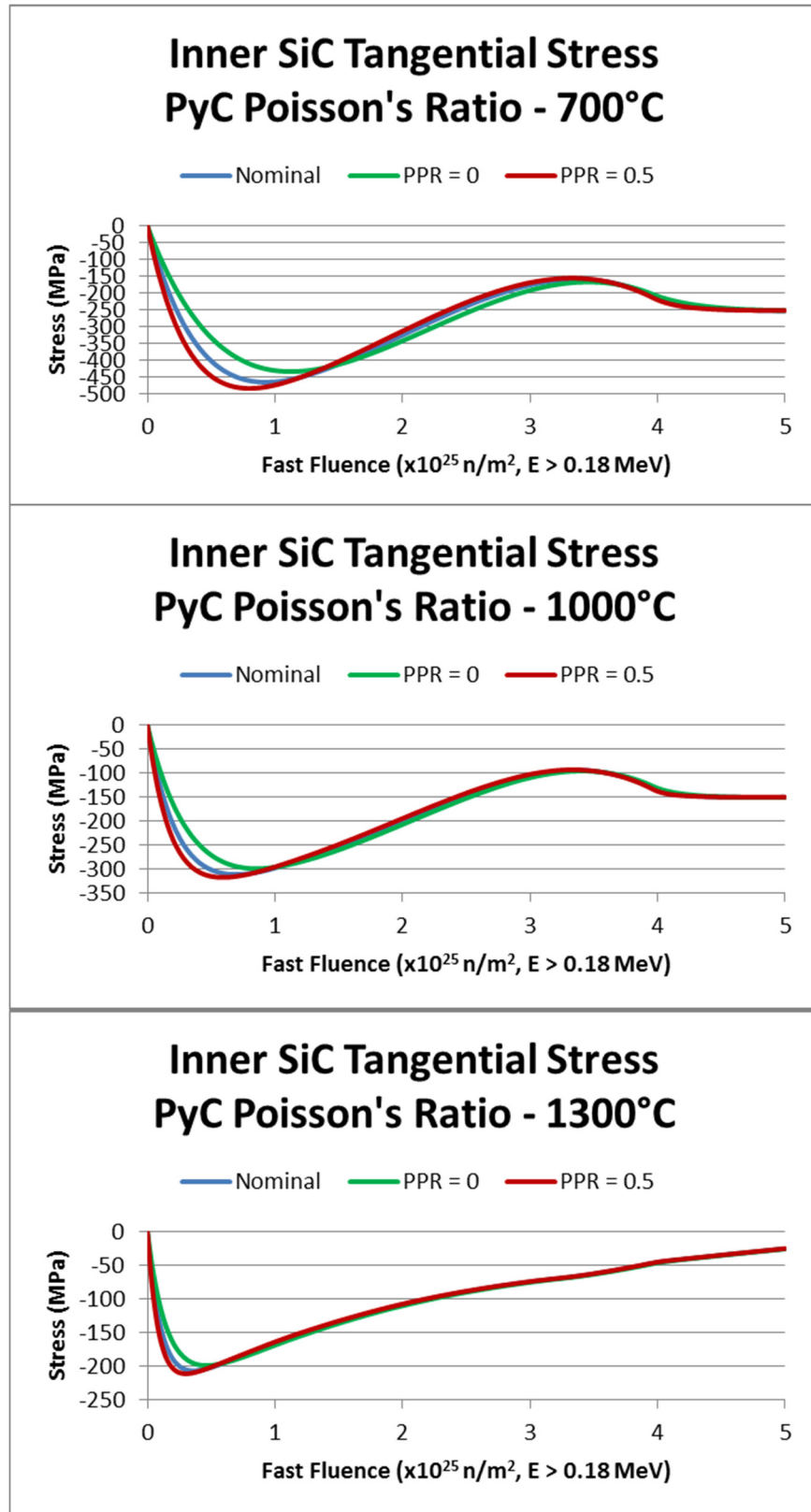
Figure 6. Tangential stress at the inner surface of the SiC layer for the nominal PyC Poisson's ratio and values 0 and 0.5.

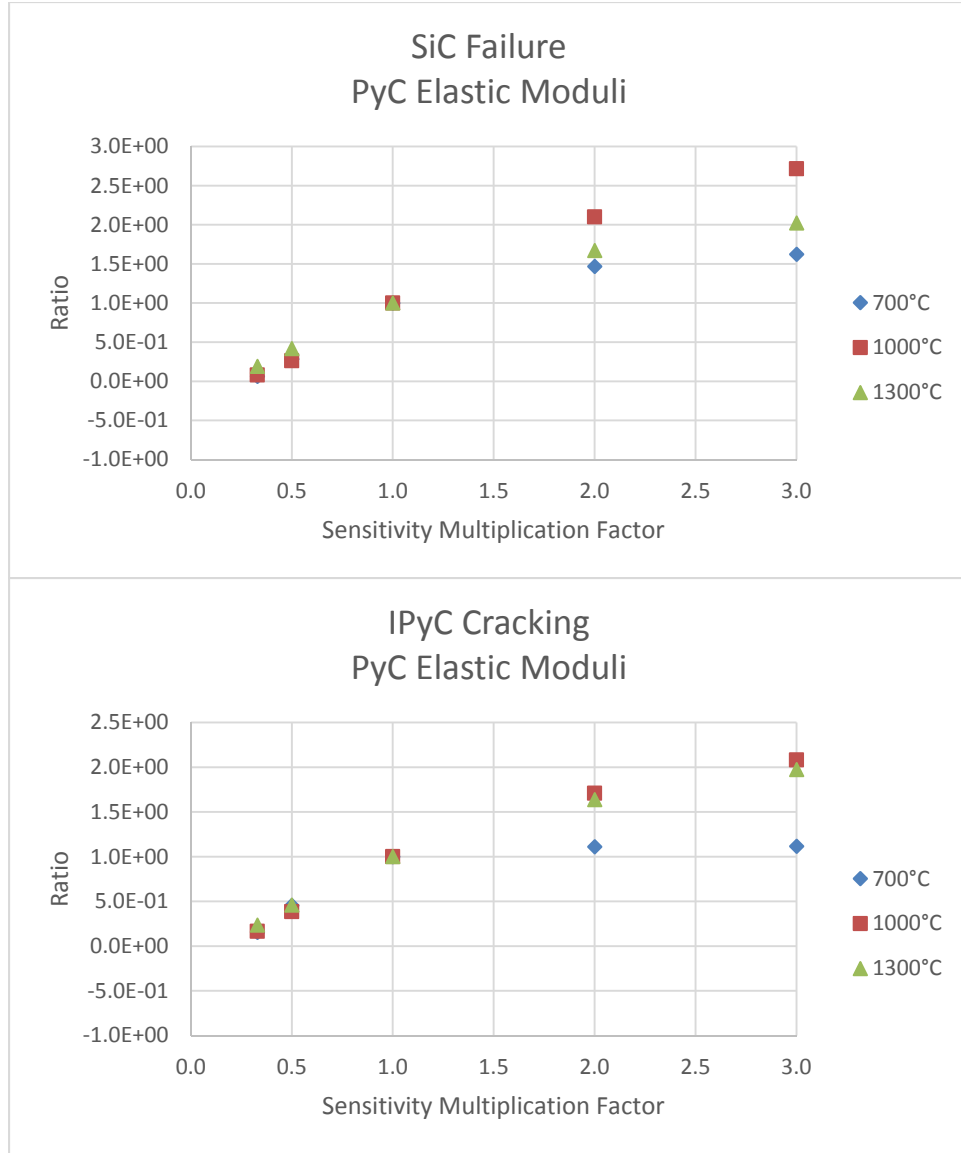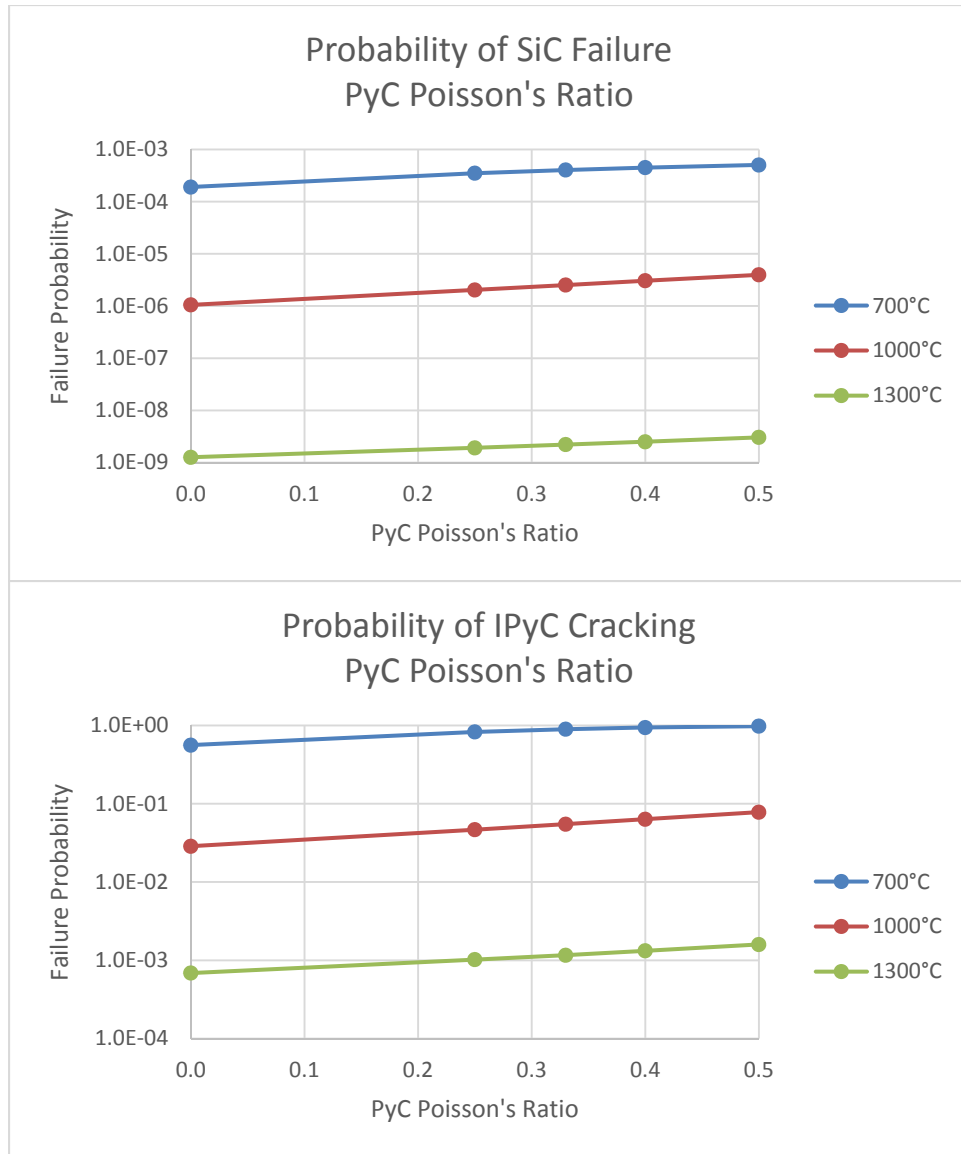Figure 7. Probability of SiC failure (top) and IPyC cracking (bottom) as a function of the value of the PyC Poisson's ratio.

Figure 8. Ratio between the probability of SiC failure (top) and IPyC cracking (bottom) values and their nominal values as a function of the value of the PyC Poisson's ratio.

7.3 Irradiation-induced Creep

The irradiation-induced creep of the PyC (K_S) is given by:

$$K_S = C_{amp} \times [1 + 2.38 \times (1.9 - \rho)]$$
$$\times (2.193 \times 10^{-4} - 4.85 \times 10^{-7} \times T + 4.0147 \times 10^{-10} \times T^2) \qquad \times 10^{-25} (\text{MPa-n/m}^2)^{-1}, \text{ T in } °C$$

The irradiation-induced creep consists of two components, transient creep and steady-state creep. Transient creep is not explicitly detailed in PARFUME because it is much smaller than steady-state creep (CEGA, 1993). A creep-amplification coefficient, C_{amp} is used in PARFUME to vary the amplitude of the irradiation-induced creep to account for uncertainty in its value. It was implemented in PARFUME with a default value ($C_{amp} = 2$) to better match experimental data from the New Production Reactor program. The steady-state creep varies with density and temperature. In these calculations, the irradiation-induced creep

coefficient of the PyC layers varies from about 1.2 to 6.4×10^{-29} $(\text{MPa-n/m}^2)^{-1}$. This range can be reduced or amplified by adjusting the coefficient C_{amp}.

Review of literature

FZJ and BNFL fuel performance modeling codes use constant irradiation-induced creep values of 1.5 and 4.8×10^{-29} $(\text{MPa-n/m}^2)^{-1}$ at all temperatures, respectively (I-NERI, 2004). Furthermore, Price and Bokros (1967) report an irradiation-induced creep constant of 1.3×10^{-29} $(\text{MPa-n/m}^2)^{-1}$ while Buckley et al. (1975) suggest a range of 3.3 to 4.9×10^{-29} $(\text{MPa-n/m}^2)^{-1}$. Morgand (1975) gives a value of 13.4×10^{-29} $(\text{MPa-n/m}^2)^{-1}$ that is deemed too high.

Range of variation

Overall range of variation: $1.2–13.4 \times 10^{-29}(\text{MPa-n/m}^2)^{-1}$

PARFUME range: $1.2–6.4 \times 10^{-29}(\text{MPa-n/m}^2)^{-1}$

Sensitivity study

Applying SMFs to the irradiation-induced creep of the PyC, Table 15 shows its impact on the failure probability of TRISO fuel under the irradiation conditions of Table 1. Figure 9 shows the tangential stress at the inner surface of the SiC layer for the nominal PyC irradiation-induced creep and SMF 0.2 and 5.

Figure 9 shows that a decrease in the irradiation-induced creep of the PyC leads to a large increase of the compressive tangential stress in the SiC layer. As seen in Table 15, this also translates into an increase of the probabilities of IPyC cracking and SiC failure. These trends can be seen in Figure 10, which plots the results of Table 15. At higher temperatures (1300°C) and high creep, the probability of SiC failure is dominated by pressure rather than IPyC cracking.

Figure 11 shows the ratio of the probabilities of Table 15 to the nominal probabilities of Table 3. It shows that the probability of SiC failure can increase by six orders of magnitude at 1300°C when the irradiation-induced creep of the PyC is reduced from its nominal value by a factor 5. The increase is less drastic at lower irradiation temperatures.

Table 15. Failure probability: PyC irradiation-induced creep.

Condition	Sensitivity Multiplication Factor	Probability of SiC failure	Probability of IPyC cracking
1	0.2	2.48×10^{-1}	9.99×10^{-1}
	0.33	5.07×10^{-2}	9.99×10^{-1}
	0.5	1.01×10^{-2}	9.99×10^{-1}
	1 (nominal)	4.03×10^{-4}	8.94×10^{-1}
	2	1.49×10^{-7}	1.06×10^{-2}
	3	5.35×10^{-10}	3.50×10^{-4}
	5	3.35×10^{-13}	3.99×10^{-6}
2	0.2	5.57×10^{-2}	9.99×10^{-1}
	0.33	7.80×10^{-3}	9.99×10^{-1}
	0.5	1.24×10^{-3}	9.99×10^{-1}
	1 (nominal)	2.52×10^{-6}	5.48×10^{-2}
	2	1.76×10^{-10}	1.57×10^{-4}
	3	4.96×10^{-13}	4.32×10^{-6}
	5	2.52×10^{-16}	4.22×10^{-8}
3	0.2	7.50×10^{-3}	9.99×10^{-1}
	0.33	7.00×10^{-4}	9.98×10^{-1}
	0.5	2.43×10^{-5}	2.73×10^{-1}
	1 (nominal)	2.21×10^{-9}	1.16×10^{-3}
	2	2.88×10^{-8}	3.04×10^{-6}
	3	2.98×10^{-7}	8.34×10^{-8}
	5	1.30×10^{-6}	8.12×10^{-10}
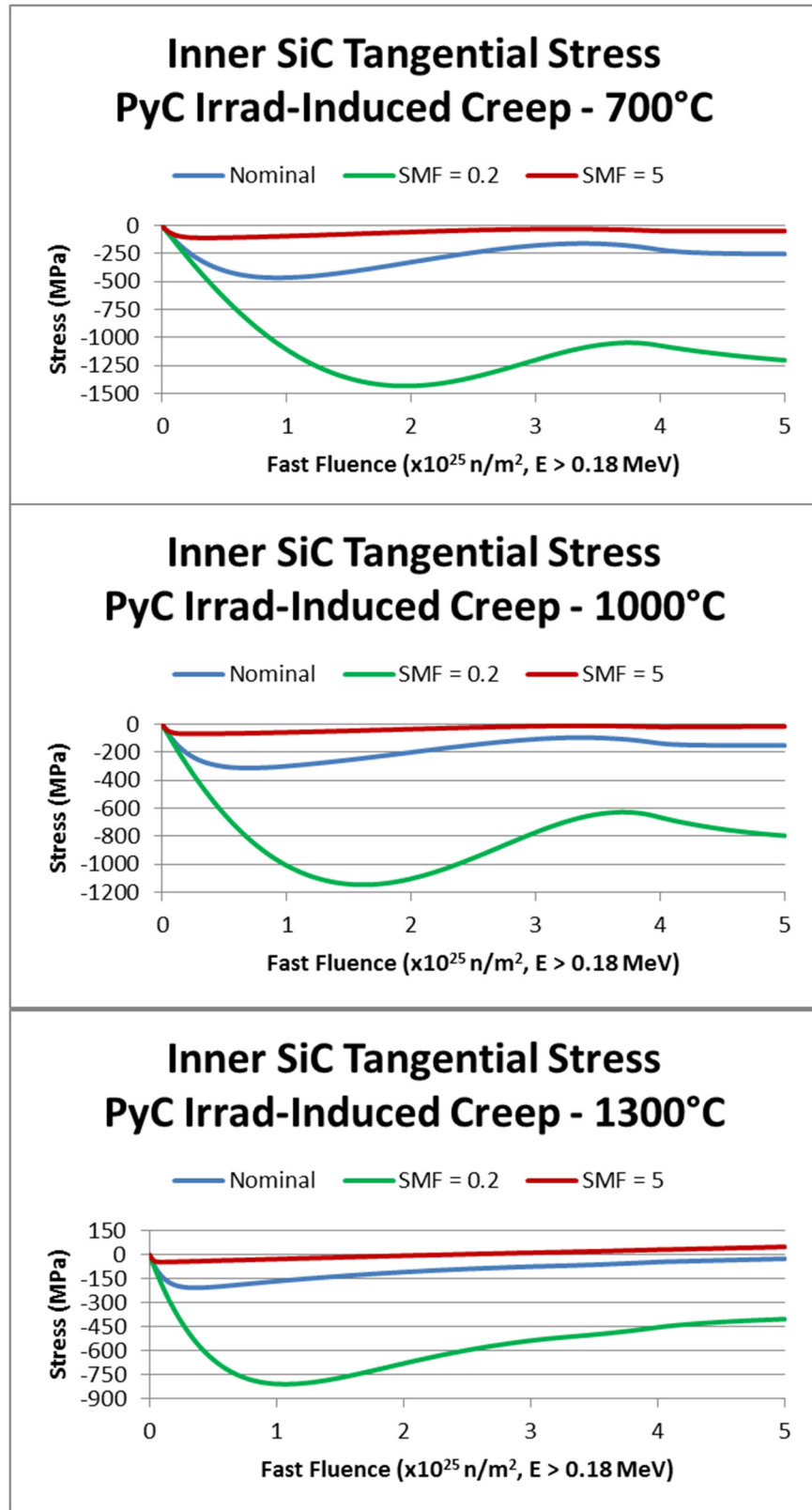
Figure 9. Tangential stress at the inner surface of the SiC layer for the nominal PyC irradiation-induced creep and SMF 0.2 and 5.

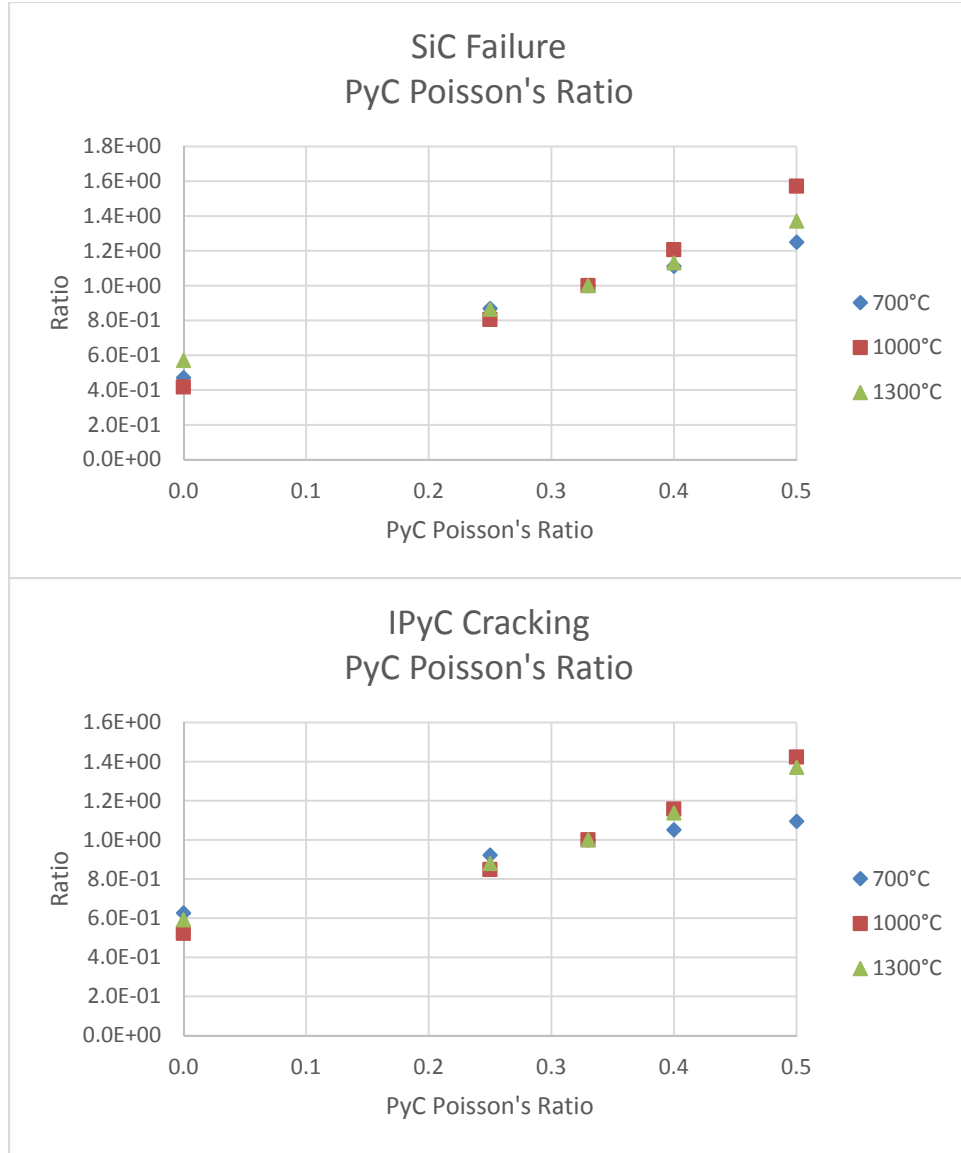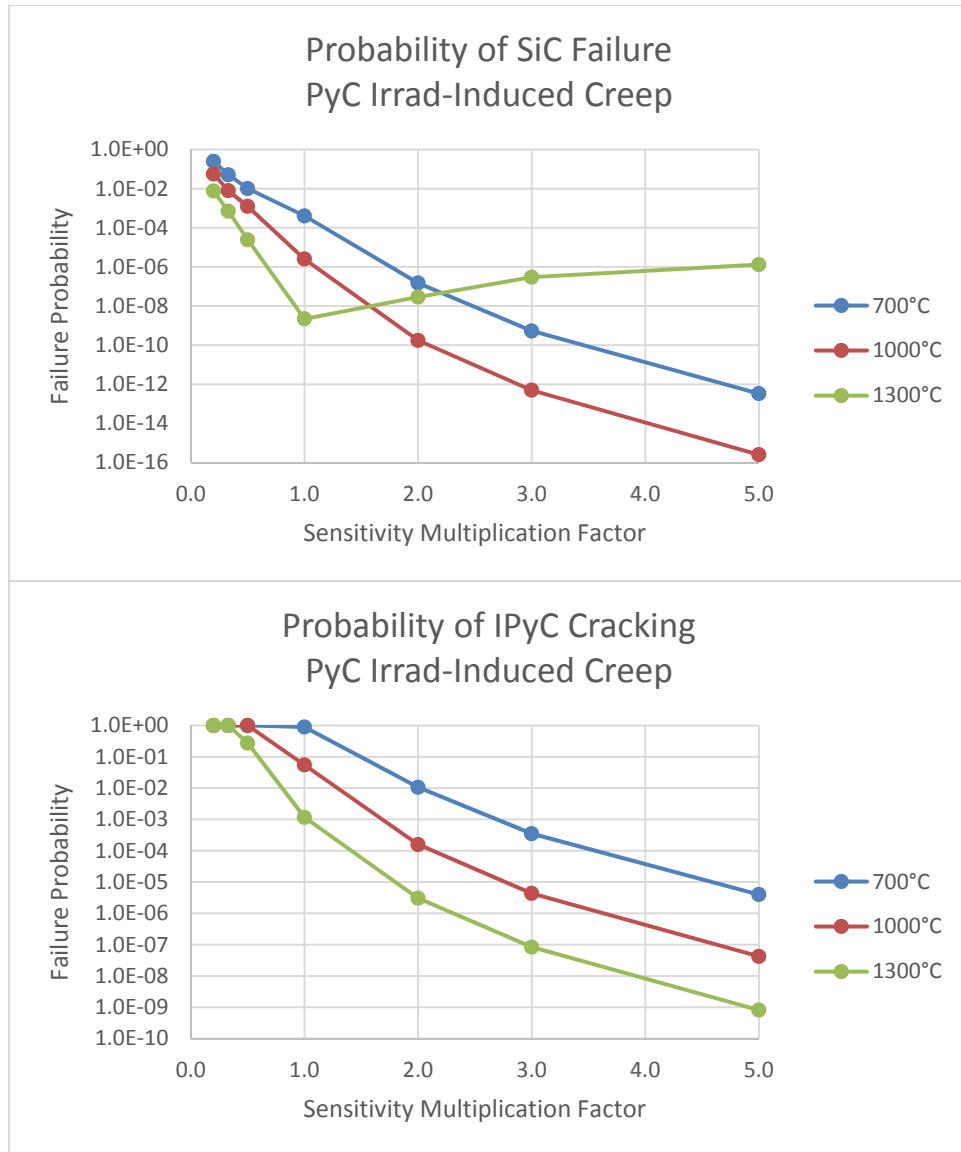Figure 10. Probability of SiC failure and IPyC cracking as a function of the sensitivity multiplication factor applied to the PyC irradiation-induced creep.

Figure 11. Ratio of the probability of SiC failure and IPyC cracking values to their nominal values as a function of the sensitivity multiplication factor applied to the PyC irradiation-induced creep.

7.4 Poisson's Ratio in Creep

The Poisson's ratio in creep of the PyC (ν) is given by:

$$\nu = 0.5$$

It is assumed constant during irradiation.

Review of literature

Kaae (1970) reports 0.33 to 0.5, while Kaae (1973) recommends a value of 0.4 at low fast fluence and 0.5 at high fast fluence. The FZJ and BNFL models use values of 0.5 and 0.4, respectively.

Range of variation

Overall range of variation: 0–0.5

PARFUME value: 0.5

Sensitivity study

Assuming values of the Poisson's ratio in creep between 0 and 0.5, Table 16 shows its impact on the failure probability of TRISO fuel under the irradiation conditions of Table 1. Figure 12 shows the tangential stress at the inner surface of the SiC layer for the nominal PyC Poisson's ratio in creep and additional values 0 and 0.25.

Figure 12 and Table 16 show that a decrease in the PyC Poisson's ratio in creep decreases the compressive stress in the SiC layer and the probabilities of IPyC cracking and SiC failure. These trends can be seen in Figure 13, which plots the results of Table 16. At higher temperatures (1300°C) and low Poisson's ratio in creep, the probability of SiC failure is dominated by pressure rather than IPyC cracking.

Figure 14 shows the ratio of the probabilities of Table 16 to the nominal probabilities of Table 3. It shows that the probability of SiC failure can decrease by up to two orders of magnitude when the Poisson's ratio in creep is reduced by a factor of 2, albeit well below values that have been measured.

Table 16. Failure probability: PyC Poisson's ratio in creep.

Condition	Poisson's ratio	Probability of SiC failure	Probability of IPyC cracking
1	0	4.88×10^{-7}	1.15×10^{-3}
	0.25	1.07×10^{-5}	2.41×10^{-2}
	0.4	1.15×10^{-4}	2.51×10^{-1}
	0.5 (nominal)	4.03×10^{-4}	8.94×10^{-1}
2	0	6.29×10^{-10}	1.61×10^{-5}
	0.25	1.63×10^{-8}	3.99×10^{-4}
	0.4	2.44×10^{-7}	5.64×10^{-3}
	0.5 (nominal)	2.52×10^{-6}	5.48×10^{-2}
3	0	7.83×10^{-10}	3.00×10^{-7}
	0.25	7.08×10^{-11}	7.63×10^{-6}
	0.4	2.01×10^{-10}	1.11×10^{-4}
	0.5 (nominal)	2.21×10^{-9}	1.16×10^{-3}
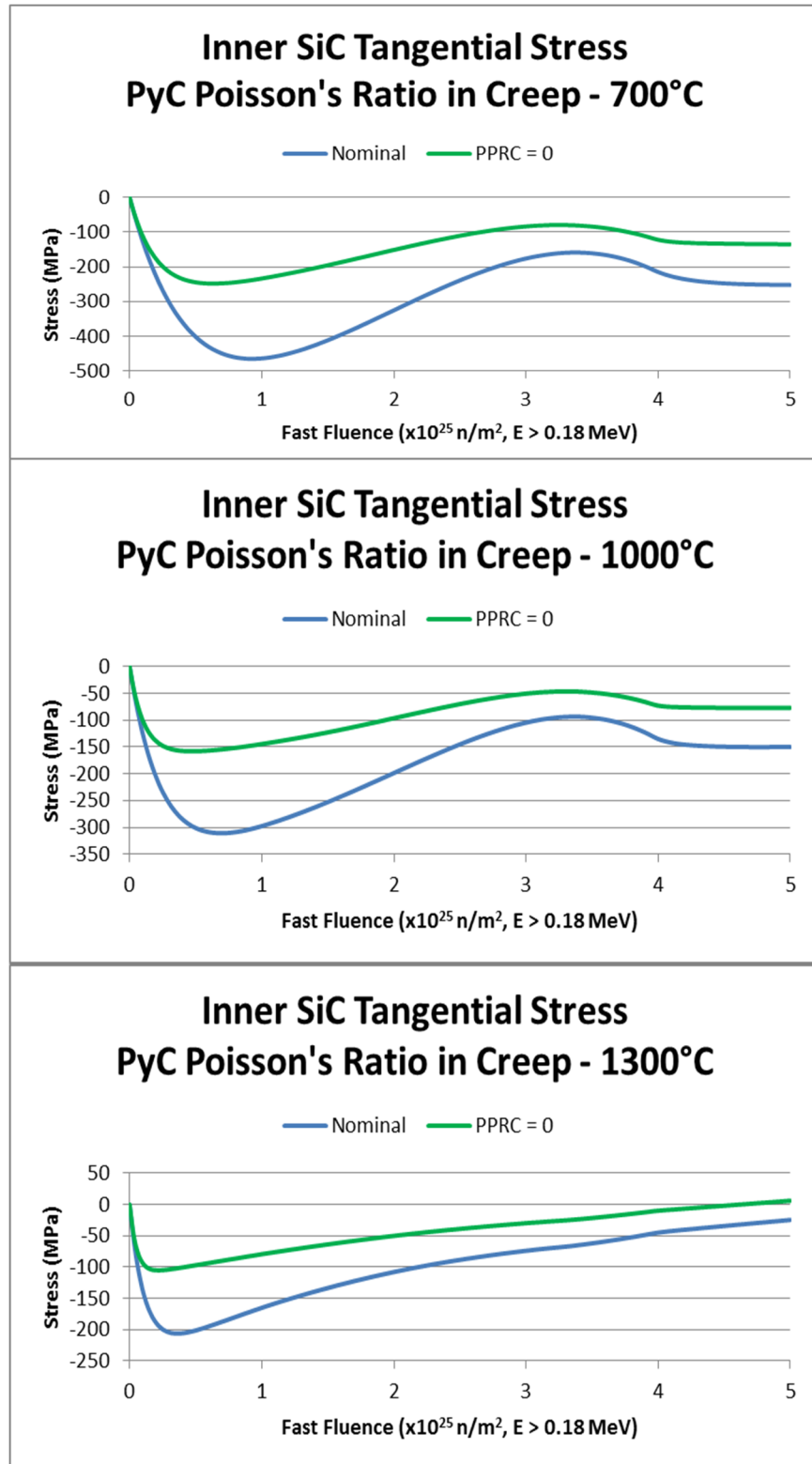
Figure 12. Tangential stress at the inner surface of the SiC layer for the nominal PyC Poisson's ratio in creep and a value of 0.

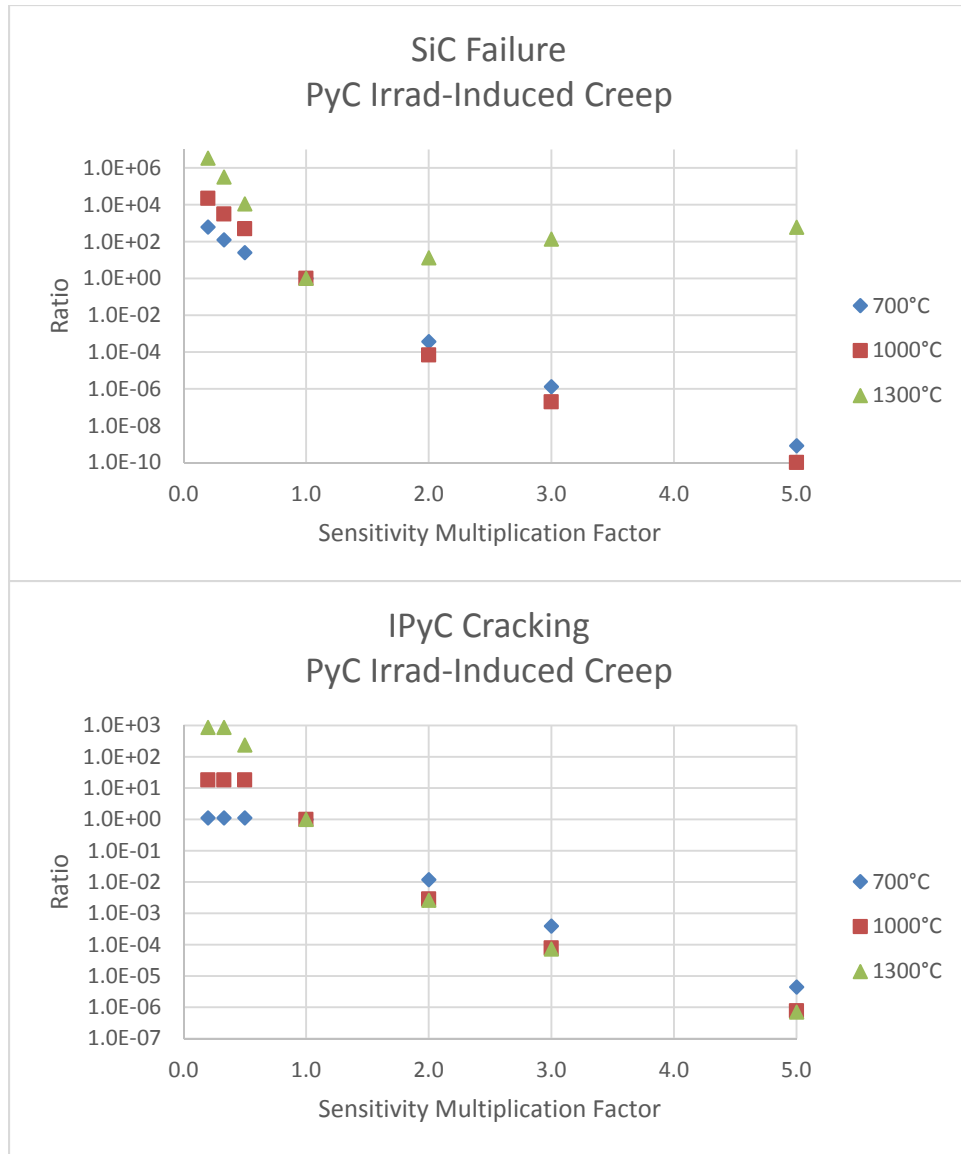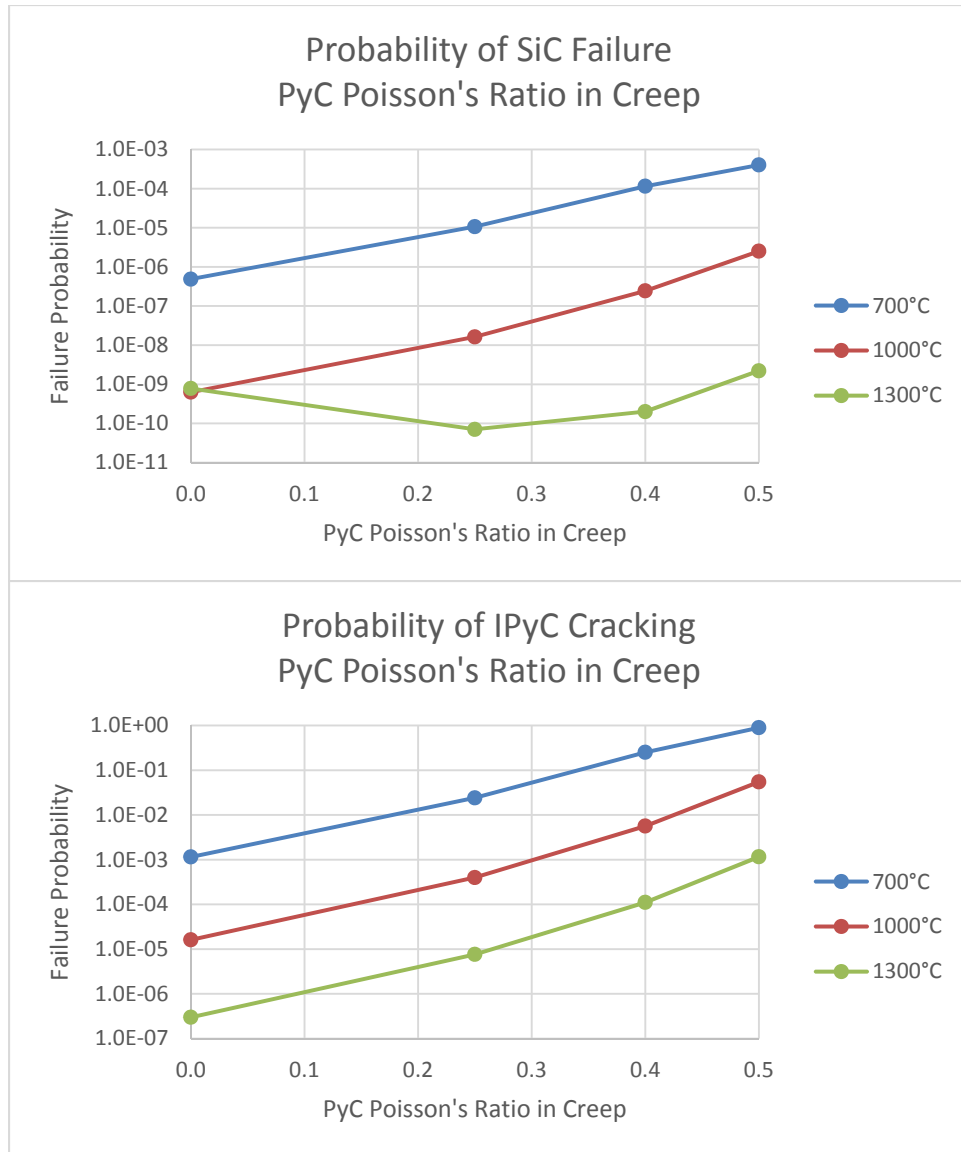Figure 13. Probability of SiC failure and IPyC cracking as a function of the value of the PyC Poisson's ratio in creep.
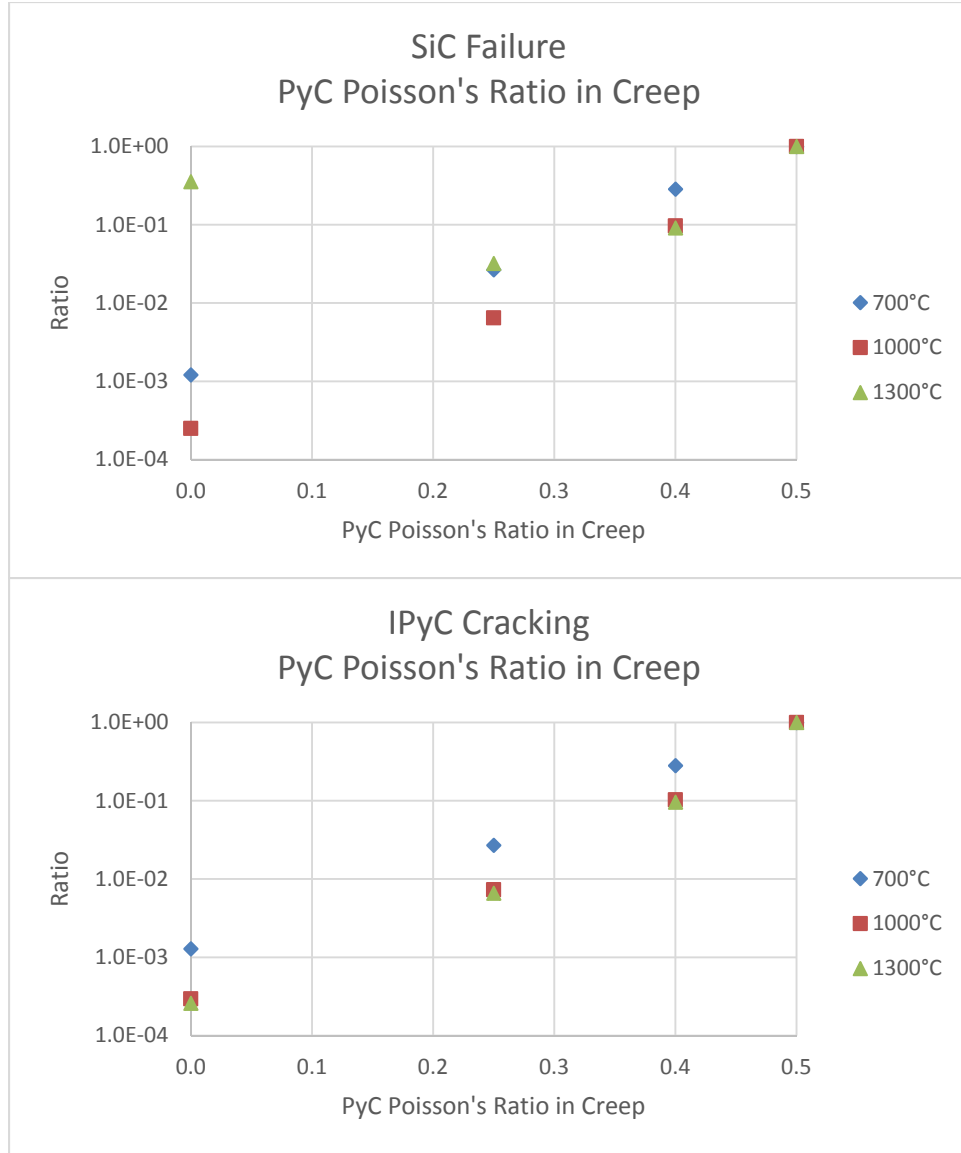
Figure 14. Ratio of the probability of SiC failure and IPyC cracking values to their nominal values as a function of the value of the PyC Poisson's ratio in creep.

7.5 Irradiation-induced Dimensional Change and Strain Rate

The irradiation-induced strain rate of the PyC ($\dot{\varepsilon}$) is given by:

$$\dot{\varepsilon} = \frac{d\varepsilon}{d\Phi} = b_0 + b_1 \times \Phi + b_2 \times \Phi^2 + b_3 \times \Phi^3 \quad \times (10^{25}\text{n/m}^2)^{-1}$$

where the b_i coefficients depend on BAF, density, and temperature, with one set of coefficients for radial strain and another for tangential strain. The PyC strains are obtained by integrating the strain rates over fast fluence; the resulting coefficients are detailed in the CEGA report and in the *PARFUME Theory and Model Basis Report*. These correlations were obtained by compiling extensive U.S. data at various BAF, densities, temperatures, and fast fluences (CEGA, 1993). Figure 15 shows the variation of the PyC radial and tangential strain rates and strains with fast fluence for an initial density of 1.9 g/cm^3 and initial BAF of 1.05 at two extremum temperatures. In these calculations, the PyC strain rates vary from -0.023 to +0.028 $\times (10^{25}\text{n/m}^2)^{-1}$ radially and from -0.030 to -0.004 $\times (10^{25}\text{n/m}^2)^{-1}$ tangentially. The PyC radial and

tangential stain rates have a cut-off in fast fluence at 4×10^{25} n/m^2. For fast fluences higher than the cut-off, the PyC strain rates keep their values at the cut-off.
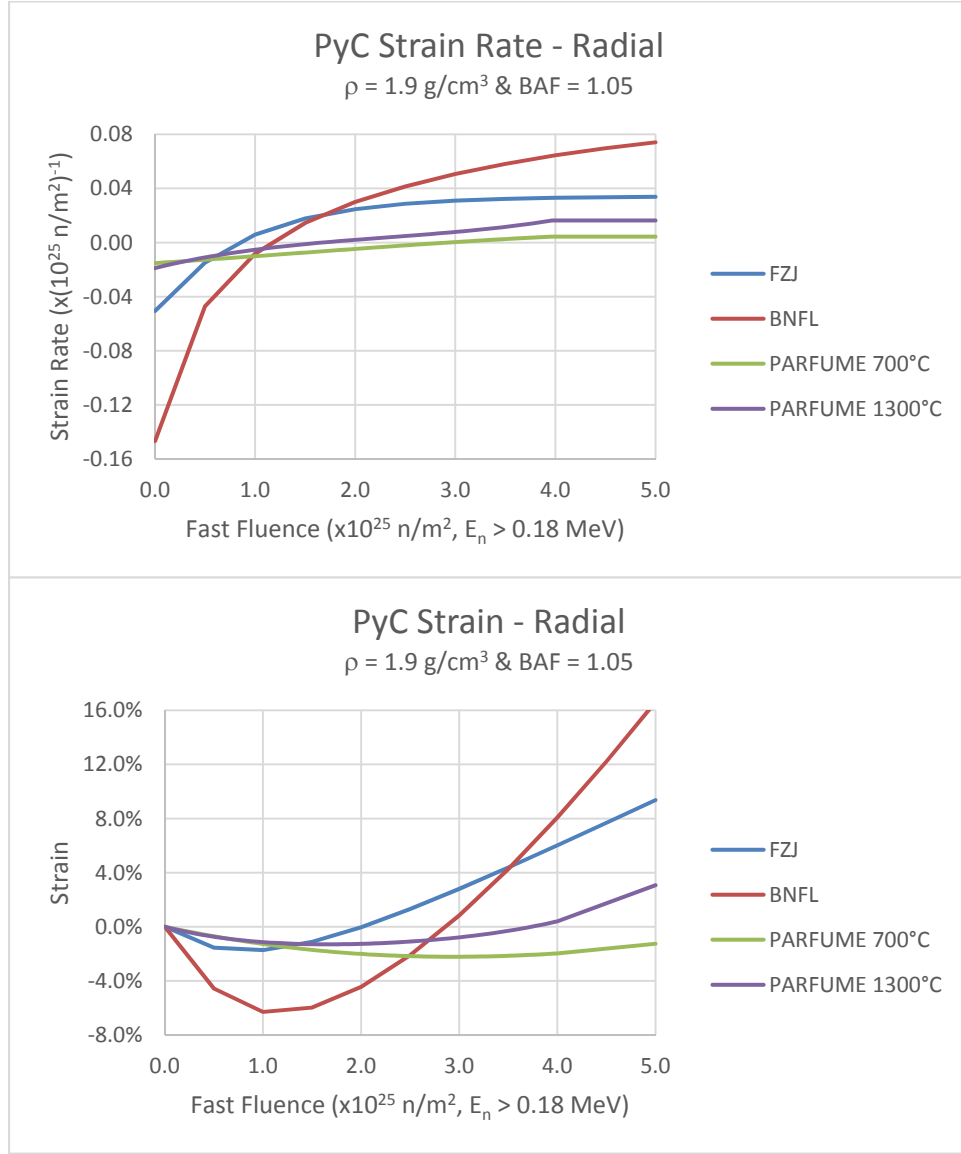
Figure 15. PyC radial strain rates and strain used in PARFUME along with BNFL, and FZJ correlations. A negative strain denotes shrinkage, while a positive strain denotes swelling.

Review of literature

In addition to the CEGA correlations, Figure 16 also shows the PyC strain rates and strains used in FZJ and BNFL fuel performance modeling codes (I-NERI, 2004). The FZJ and BNFL correlations are not density or BAF specific and their corresponding strain rates only vary with fluence. In these calculations, the radial and tangential strain rates for these three correlations vary from -0.147 to +0.074$\times(10^{25}$n/m$^2)^{-1}$ and from -0.051 to +0.001$\times(10^{25}$n/m$^2)^{-1}$, respectively.
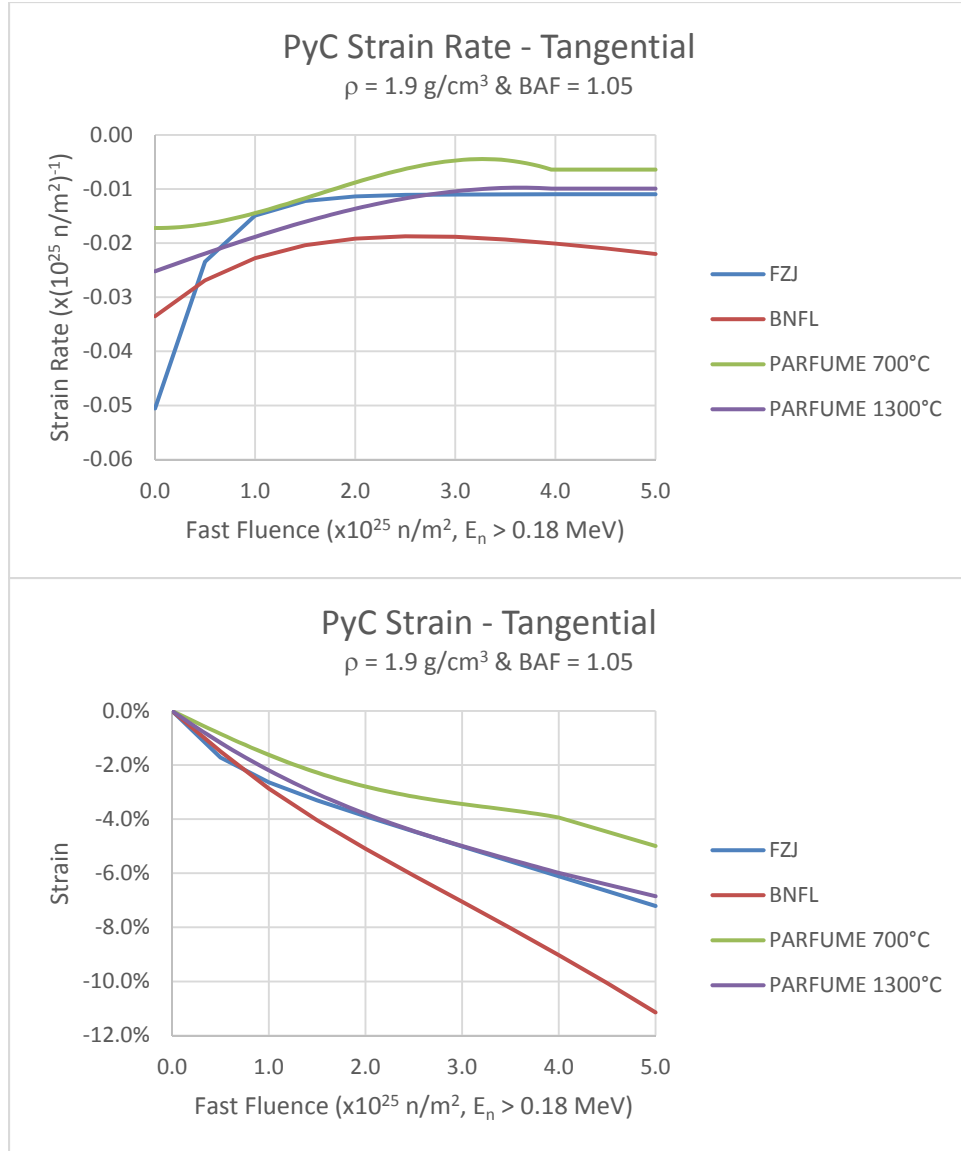
Figure 16. PyC tangential strain rates and strain used in PARFUME along with BNFL and FZJ correlations. A negative strain denotes shrinkage, while a positive strain denotes swelling.

Range of variation

Overall range of variation: -0.147–$0.074 \times (10^{25} n/m^2)^{-1}$ radial
-0.051–$0.001 \times (10^{25} n/m^2)^{-1}$ tangential

PARFUME value: -0.023–$0.028 \times (10^{25} n/m^2)^{-1}$ radial
-0.030– $-0.004 \times (10^{25} n/m^2)^{-1}$ tangential

Sensitivity study

Applying SMF that bound the range of variation of the PyC strain rates, Table 17 shows the impact of the irradiation-induced dimensional change in the PyC layer on the failure probability of TRISO fuel under the irradiation conditions of Table 1. Figure 17 shows the tangential stress at the inner surface of the SiC layer for the nominal buffer strain rate and SMF 0.2 and 5.

Figure 17 shows that an increase in the magnitude of the PyC strain rates leads to a large increase of the compressive tangential stress in the SiC layer. As seen in Table 17, this also translates into an increase

of the probabilities of IPyC cracking and SiC failure. This trend can be seen in Figure 18 that plots the results of Table 17. At higher temperatures (1300°C) and low strain rates, the probability of SiC failure is dominated by pressure rather than IPyC cracking.

Figure 19 shows the ratio of the probabilities of Table 17 to the nominal probabilities of Table 3. It shows that the probability of SiC failure can increase by seven orders of magnitude at 1300°C when the PyC strain rates are multiplied by a factor of five, albeit well beyond historical measurements of these strain rates. Although the initial shrinkage of the IPyC layer puts the SiC in compression and prevents its inner tangential stress to become tensile and fail the layer, excessive shrinkage increases the probability of IPyC cracking. A radial crack in the IPyC layer results in local tensile stress in the SiC layer, which increases its probability of failure. The increase is less drastic at lower irradiation temperatures.

Table 17. Failure probability: PyC irradiation-induced dimensional change.

Condition	Sensitivity Multiplication Factor	Probability of SiC failure	Probability of IPyC cracking
1	0.2	1.66×10^{-14}	5.34×10^{-7}
	0.33	3.98×10^{-11}	6.27×10^{-5}
	0.5	2.52×10^{-8}	3.27×10^{-3}
	1 (nominal)	4.03×10^{-4}	8.94×10^{-1}
	2	2.76×10^{-2}	9.99×10^{-1}
	3	2.57×10^{-1}	9.99×10^{-1}
	5	9.68×10^{-1}	9.99×10^{-1}
2	0.2	3.66×10^{-17}	1.25×10^{-8}
	0.33	8.82×10^{-14}	1.48×10^{-6}
	0.5	5.58×10^{-11}	7.75×10^{-5}
	1 (nominal)	2.52×10^{-6}	5.48×10^{-2}
	2	2.59×10^{-3}	9.99×10^{-1}
	3	2.89×10^{-2}	9.99×10^{-1}
	5	4.21×10^{-1}	9.99×10^{-1}
3	0.2	1.87×10^{-6}	2.49×10^{-10}
	0.33	3.96×10^{-7}	3.00×10^{-8}
	0.5	3.20×10^{-8}	1.58×10^{-6}
	1 (nominal)	2.21×10^{-9}	1.16×10^{-3}
	2	6.38×10^{-5}	5.65×10^{-1}
	3	1.19×10^{-3}	9.99×10^{-1}
	5	2.48×10^{-2}	9.99×10^{-1}
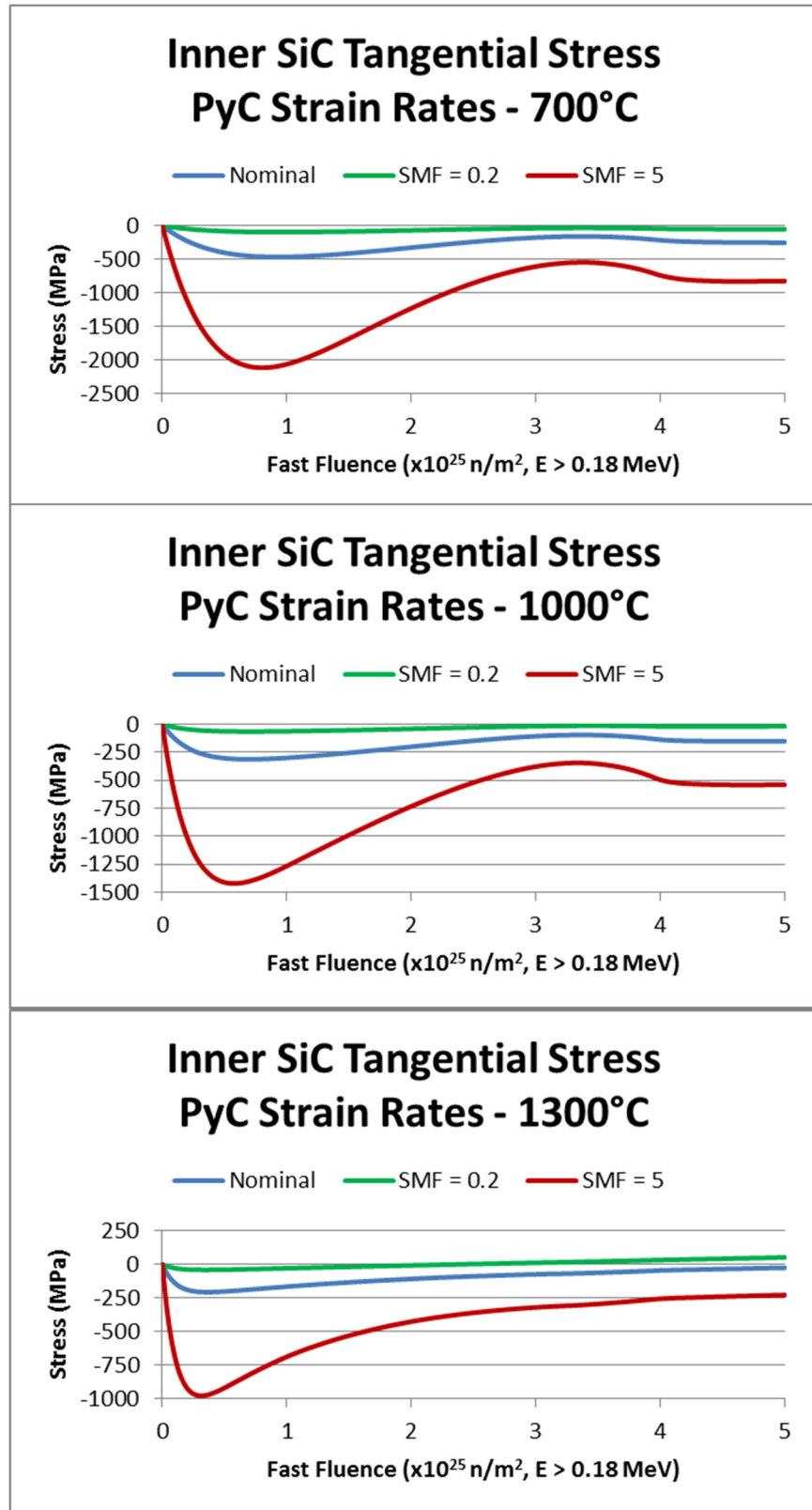
Figure 17. Tangential stress at the inner surface of the SiC layer for the nominal PyC strain rates and SMF 0.2 and 5.
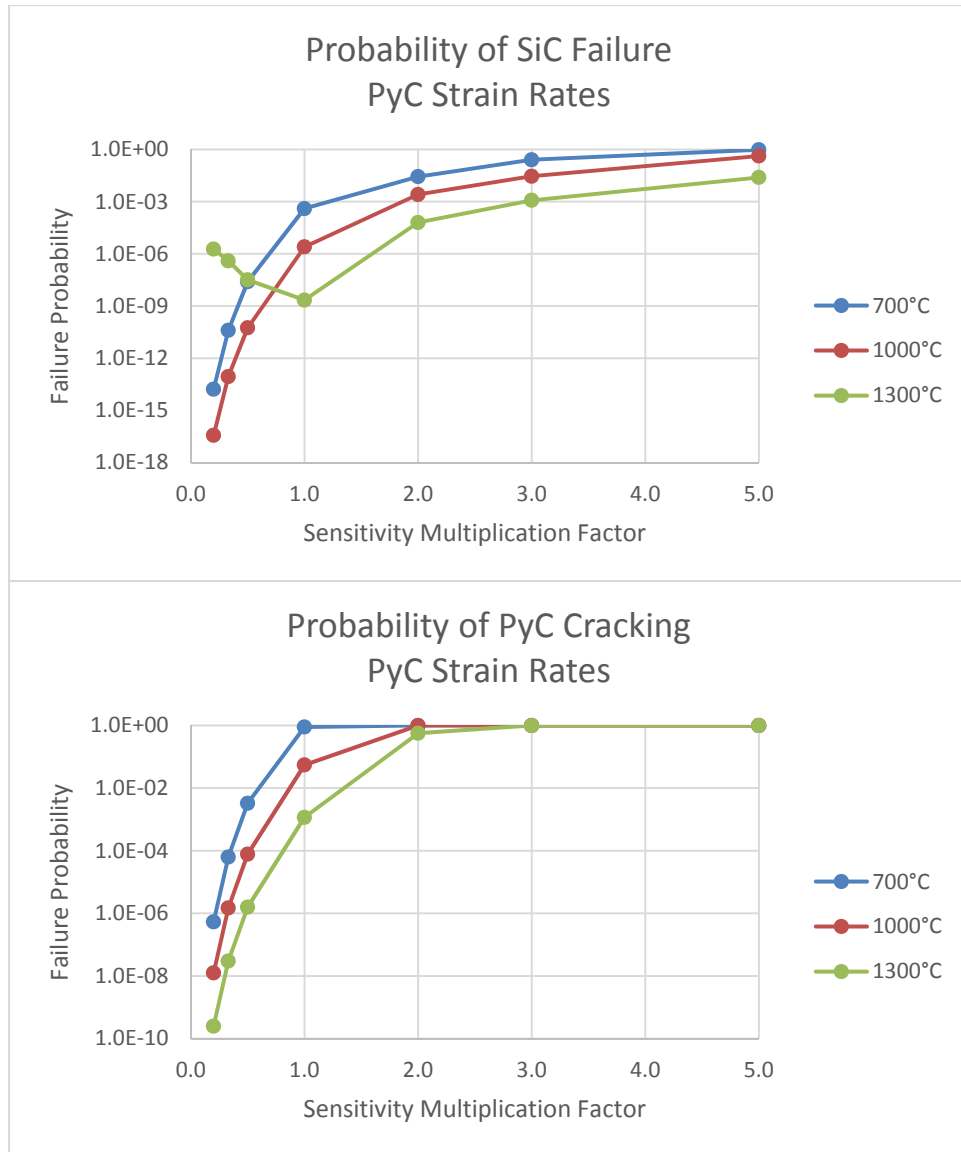
Figure 18. Probability of SiC failure and IPyC cracking as a function of the sensitivity multiplication factor applied to the PyC strain rates.
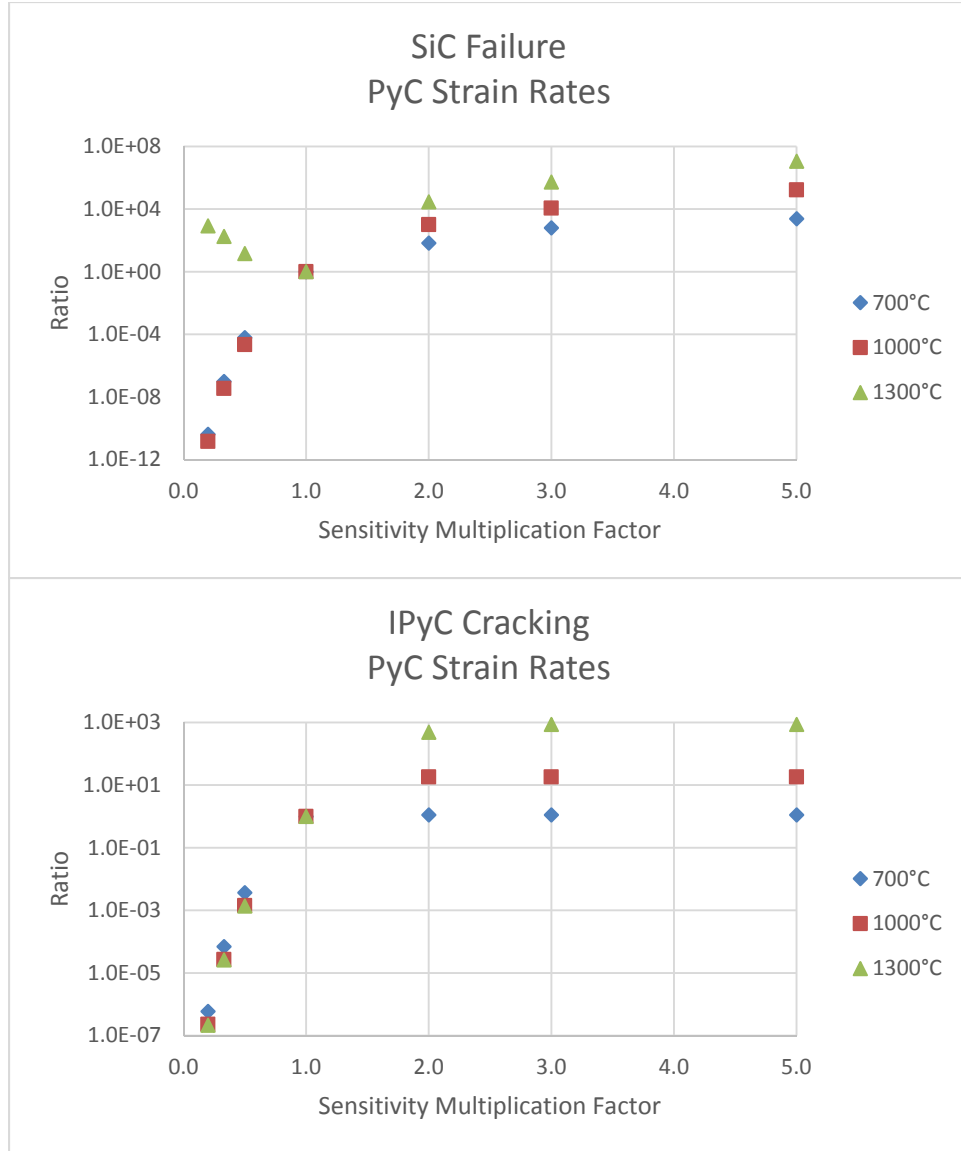
Figure 19. Ratio of the probability of SiC failure and IPyC cracking values to their nominal values as a function of the sensitivity multiplication factor applied to the PyC strain rates.

7.6   Weibull characteristic strength and modulus

In Weibull theory, the failure probability of a coating layer is expressed as:

$$P_f = 1 - \int_V \left(\frac{\sigma}{\sigma_o}\right)^m dV$$

which calculates the probability of the tensile stress (σ) in the volume (V) of that layer to be greater than its characteristic strength (σ_o). The Weibull modulus (m) describes the variability in measured strength. The Weibull characteristic strength and modulus of the PyC are given by:

$\sigma_0 = 16.8$ MPa-m$^{3/m}$
$m = 9.5$

The PyC Weibull parameters are described in the CEGA report. In PARFUME, the PyC Weibull modulus is assumed to remain constant throughout irradiation and independent of temperature or fast fluence, whereas the PyC characteristic strength is fast fluence- and temperature-dependent.

Review of literature

Kaae et al. (1977) reported three-point bending measurements of Weibull parameters of propylene-derived PyC. The CEGA report used these results to perform a regression analysis that indicated that the value of the modulus decreases from ~11 at a density of 1.8 g/cm^3 to ~8 at a density of 2 g/cm^3. A mean value of 9.5 was then chosen. This analysis also showed that the PyC Weibull modulus is not very sensitive to BAF. Using the same results, the CEGA report determined the associated PyC characteristic strengths: 10.0 MPa-m$^{3/8}$, 16.8 MPa-m$^{3/9.5}$, and 24.5 MPa-m$^{3/11}$.

Range of variation

Overall range of variation: m = 8 and σ_0 = 10.0 MPa-m$^{3/m}$ to m = 11 and σ_0 = 24.5 MPa-m$^{3/m}$

PARFUME values: m = 9.5 and σ_0 = 16.8 MPa-m$^{3/m}$

Sensitivity study

Assuming the PyC Weibull modulus varies between 8 and 11, the corresponding values of the PyC characteristic strength vary from 10.0 to 24.5 MPa-m$^{3/m}$. Table 18 shows the impact of the variation of the PyC Weibull parameters on the failure probability of TRISO fuel under the irradiation conditions of Table 1.

Figure 20 shows the probability of SiC failure and IPyC cracking as a function of the PyC Weibull modulus using results from Table 18.

Figure 21 shows the ratio between the probabilities of Table 18 and the nominal probabilities of Table 3. It shows that the probability of SiC failure can quadruple when the PyC Weibull parameters are reduced at high irradiation temperature. The impact of a reduction of the PyC Weibull parameters decreases at lower irradiation temperatures.

Table 18. Failure probability: PyC Weibull parameters.

Condition	Weibull m / σ_0	Probability of SiC failure	Probability of IPyC cracking
1	8 / 10.0	4.20×10^{-4}	9.40×10^{-1}
	9.5 / 16.8 (nominal)	4.03×10^{-4}	8.94×10^{-1}
	11 / 24.5	3.76×10^{-4}	8.19×10^{-1}
2	8 / 10.0	5.37×10^{-6}	1.19×10^{-1}
	9.5 / 16.8 (nominal)	2.52×10^{-6}	5.48×10^{-2}
	11 / 24.5	1.10×10^{-6}	2.35×10^{-2}
3	8 / 10.0	9.02×10^{-9}	4.86×10^{-3}
	9.5 / 16.8 (nominal)	2.21×10^{-9}	1.16×10^{-3}
	11 / 24.5	5.13×10^{-10}	2.65×10^{-4}
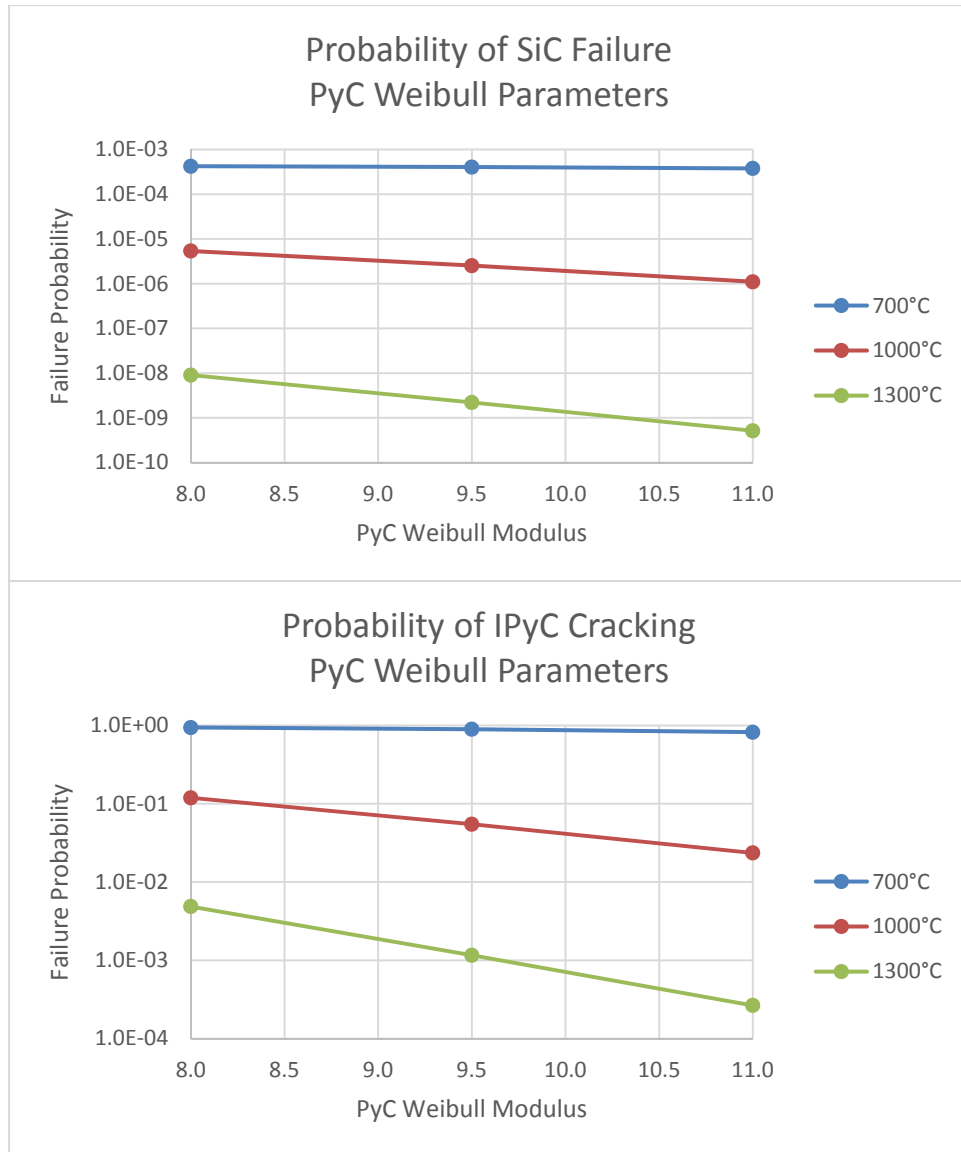
Figure 20. Probability of SiC failure and IPyC cracking as a function of the PyC Weibull modulus. Each PyC Weibull modulus corresponds the PyC characteristic strength shown in Table 18.
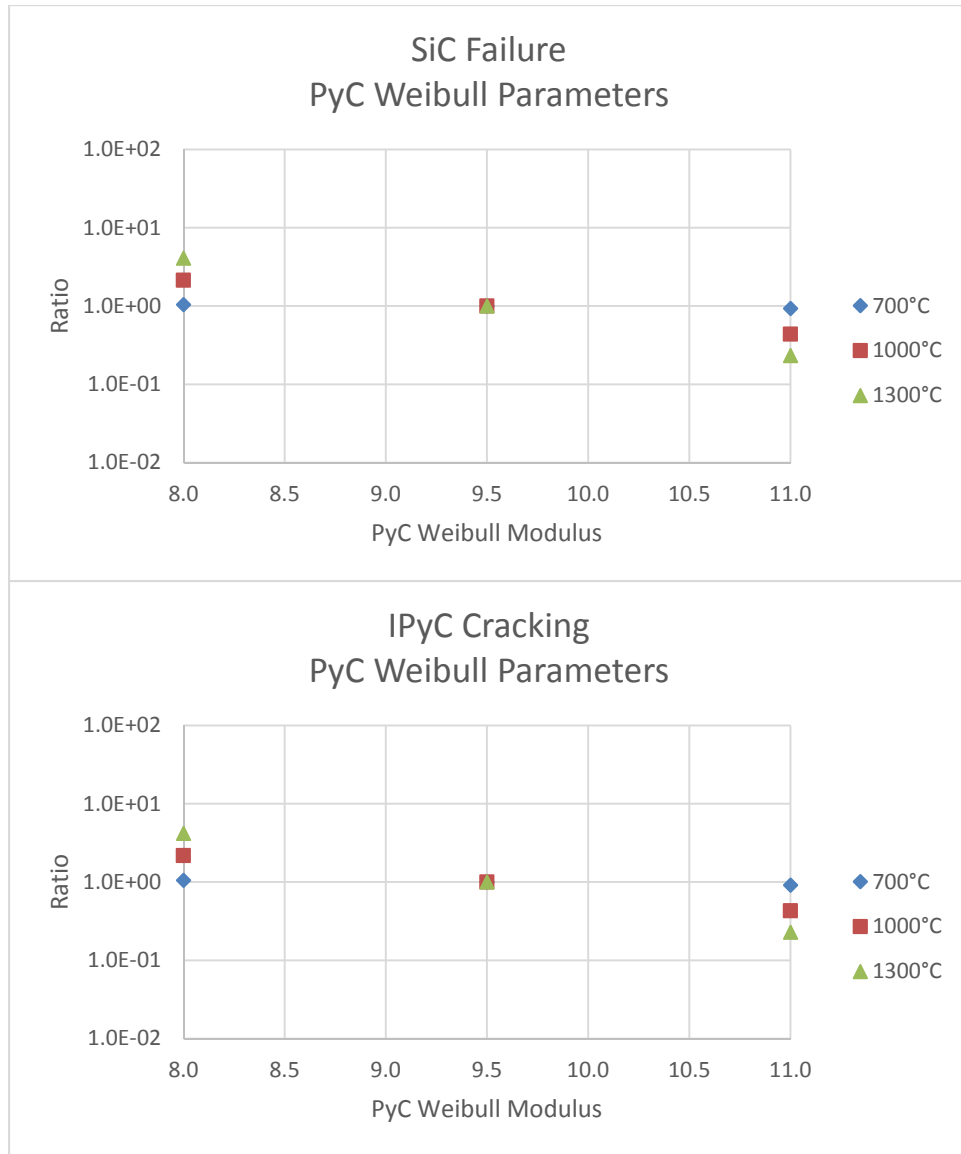
Figure 21. Ratio between the probability of SiC failure and IPyC cracking values and their nominal values as a function of the PyC Weibull modulus. Each PyC Weibull modulus corresponds the PyC characteristic strength shown in Table 18.

7.7   Thermal Conductivity

The thermal conductivity of the PyC (k) is given by:

k = 4.0 W/(m·K)

It is assumed constant over irradiation.

Review of literature

In BNFL TRISO fuel modeling, the thermal conductivity of the PyC increases with density and ranges from 6.4 to 7.8 W/(m·K) in these calculations, while FZJ fuel performance modeling codes assume a constant value of 4.0 W/(m·K) (I-NERI, 2004). Additionally, Rochais et al. (2008) performed microscopic thermal characterization of TRISO particle coating layers and measured room-temperature

conductivities of 4.8 and 10.3 W/(m·K) for IPyC and OPyC layers, respectively. Lopez-Honorato et al., (2008b) report values from 3.4 to 13.5 W/(m·K), depending on the deposition conditions, while Salgado et al. (1971) suggest values of 3.8 and 8.4 W/(m·K).

Range of variation

Overall range of variation: 3.4–13.5 W/(m·K)

PARFUME value: 4.0 W/(m·K)

Sensitivity study

Applying SMF the thermal conductivity of the PyC in PARFUME, Table 19 shows its impact of on the failure probability of TRISO fuel under the irradiation conditions of Table 1. Results show that variations of the PyC thermal conductivity have negligible impact on the probability of SiC failure.

Table 19. Failure probability: PyC thermal conductivity.

Condition	Sensitivity Multiplication Factor	Probability of SiC failure	Probability of IPyC cracking
1	0.33	4.03×10^{-4}	8.92×10^{-1}
	0.5	4.03×10^{-4}	8.93×10^{-1}
	1 (nominal)	4.03×10^{-4}	8.94×10^{-1}
	2	4.04×10^{-4}	8.94×10^{-1}
	3	4.04×10^{-4}	8.95×10^{-1}
2	0.33	2.45×10^{-6}	5.33×10^{-2}
	0.5	2.49×10^{-6}	5.40×10^{-2}
	1 (nominal)	2.52×10^{-6}	5.48×10^{-2}
	2	2.54×10^{-6}	5.51×10^{-2}
	3	2.54×10^{-6}	5.52×10^{-2}
3	0.33	2.16×10^{-9}	1.14×10^{-3}
	0.5	2.18×10^{-9}	1.15×10^{-3}
	1 (nominal)	2.21×10^{-9}	1.16×10^{-3}
	2	2.22×10^{-9}	1.17×10^{-3}
	3	2.22×10^{-9}	1.17×10^{-3}

7.8   Thermal Expansion

The thermal-expansion coefficients of the PyC in the radial (α_r) and tangential (α_t) directions are given by:

$$\alpha_r = \left(30 - 37.5 \times \frac{2}{2+BAF}\right) \times \left(1 + 0.11 \times \frac{T-400}{700}\right) \qquad \times 10^{-6}/°C, \text{ T in } °C$$
$$\alpha_t = \left(1 + 36 \times \frac{1}{(2+BAF)^2}\right) \times \left(1 + 0.11 \times \frac{T-400}{700}\right) \qquad \times 10^{-6}/°C, \text{ T in } °C$$

The coefficients of thermal expansion of the PyC in the radial and tangential directions are functions of BAF and temperature. In these calculations, they vary from 5.5 to $6.7 \times 10^{-6}/°C$ radially and from 4.9 to $5.6 \times 10^{-6}/°C$ tangentially.

Review of literature

FZJ and BNFL fuel performance modeling codes use values of 5.5 and $5.6 \times 10^{-6}/K$, respectively, (I-NERI, 2004). Price and Bokros (1967) report values between 3.9 and $5.0 \times 10^{-6}/°C$ at low temperature.

Range of variation

Overall range of variation: $3.9–6.7 \times 10^{-6}/°C$

PARFUME range: $4.9–6.7 \times 10^{-6}/°C$

Sensitivity study

Applying SMF to the thermal expansion of the PyC in PARFUME, Table 20 shows its impact on the failure probability of TRISO fuel under the irradiation conditions of Table 1. Results show that variations of the PyC thermal expansion have no impact on the probability of SiC failure. Thermal expansion of the PyC layers affects the TRISO particle only if there are appreciable temperature changes in these layers throughout irradiation, which is not the case in this study. Even though, typical temperature variations of a few hundred degrees would yield limited thermal expansion compared to dimensional changes induced by irradiation.

Table 20. Failure probability: PyC thermal expansion.

Condition	Sensitivity Multiplication Factor	Probability of SiC failure	Probability of IPyC cracking
1	0.5	4.04×10^{-4}	8.94×10^{-1}
	0.66	4.04×10^{-4}	8.93×10^{-1}
	1 (nominal)	4.03×10^{-4}	8.94×10^{-1}
	1.5	4.03×10^{-4}	8.94×10^{-1}
	2	4.03×10^{-4}	8.94×10^{-1}
2	0.5	2.52×10^{-6}	5.48×10^{-2}
	0.66	2.52×10^{-6}	5.48×10^{-2}
	1 (nominal)	2.52×10^{-6}	5.48×10^{-2}
	1.5	2.52×10^{-6}	5.47×10^{-2}
	2	2.52×10^{-6}	5.47×10^{-2}
3	0.5	2.21×10^{-9}	1.17×10^{-3}
	0.66	2.21×10^{-9}	1.17×10^{-3}
	1 (nominal)	2.21×10^{-9}	1.16×10^{-3}
	1.5	2.21×10^{-9}	1.16×10^{-3}
	2	2.20×10^{-9}	1.16×10^{-3}

7.9   Summary of the Material Properties of the PyC Layers

The material properties of the PyC layers used in PARFUME are

- Elastic moduli
- Poisson's ratio
- Irradiation-induced creep
- Poisson's ratio in creep
- Strain rates
- Weibull characteristic strength and modulus
- Thermal conductivity

- Thermal expansion.

Some of the material properties of the PyC layers (elastic moduli, irradiation-induced creep, strain rates, Weibull parameters, and thermal conductivity) exhibit large variabilities, but their subsequent impact on the probability of SiC failure is only significant for irradiation-induced creep, strain rates, Poisson's ratio in creep, and Weibull parameters.

8. MATERIAL PROPERTIES: SiC

8.1 Elastic Modulus

The elastic modulus of the SiC (E) is given by:

E = E(T)   GPa

The elastic modulus of the SiC layer in PARFUME is a function of temperature. Its values at room temperature (25°C) and elevated temperatures were obtained from Gulden (1969). Figure 22 shows its variation with temperature. At room temperature, the elastic modulus has a value of 427 GPa. In these calculations, it varies from 308 to 389 GPa.
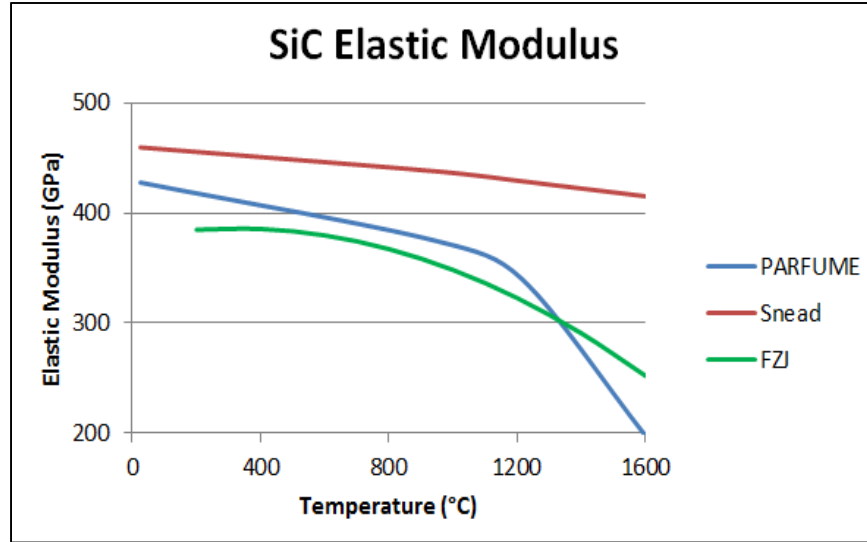
Figure 22. SiC modulus of elasticity as a function of temperature.

Review of literature

Price (1977) gives the same value of 427 GPa at room temperature, while the CEGA Corporation reports other room-temperature values that range from -50 to +40% of value reported by Gulden (CEGA, 1993). Based on nanoindentation and crush-testing techniques applied to ten different samples, Hosemann et al. (2013) report room-temperature values between 300 and 340 GPa, with two outliers at around 200 GPa. Shorter deposition time and higher flow rate in the coating process led to lower elastic moduli. Furthermore, FZJ (Freis, 2009) and Snead et al. (2007) claim a smaller reduction of the elastic modulus with temperature, as shown in Figure 18. Assuming respective variations of -50 and +40% of the values 308 and 389 GPa, the subsequent range extends from 154 to 545 GPa, encompassing the values suggested by FZJ and Snead et al.

Range of variation

Overall range of variation: 154–545 GPa

PARFUME range: 308–389 GPa

Sensitivity study

Applying SMFs to the elastic modulus of the SiC in PARFUME, Table 21 shows its impact on the failure probability of TRISO fuel under the irradiation conditions of Table 1. Figure 23 shows the tangential stress at the inner surface of the SiC layer for the nominal SiC elastic modulus and SMF 0.2 and 5.

Figure 23 shows that an increase of the SiC elastic modulus leads to an increase of the compressive tangential stress in the SiC layer. As seen in Table 21, this also translates into an increase of the probabilities of IPyC cracking and SiC failure. These trends can be seen in Figure 24, which plots the results of Table 21.

Figure 25 shows the relative difference between the probabilities of Table 21 and the nominal probabilities of Table 3. It shows that the probability of SiC failure increases by a maximum of 70% when the elastic modulus of the SiC is multiplied by a factor 5, albeit well beyond any values available in the literature.

Table 21. Failure probability: SiC elastic modulus.

Condition	Sensitivity Multiplication Factor	Probability of SiC failure	Probability of IPyC cracking
1	0.2	4.73×10^{-5}	4.45×10^{-1}
	0.5	2.31×10^{-4}	7.95×10^{-1}
	1 (nominal)	4.03×10^{-4}	8.94×10^{-1}
	2	5.40×10^{-4}	9.31×10^{-1}
	5	6.45×10^{-4}	9.49×10^{-1}
2	0.2	2.92×10^{-7}	2.12×10^{-2}
	0.5	1.39×10^{-6}	4.29×10^{-2}
	1 (nominal)	2.52×10^{-6}	5.48×10^{-2}
	2	3.46×10^{-6}	6.23×10^{-2}
	5	4.21×10^{-6}	6.71×10^{-2}
3	0.2	5.10×10^{-10}	4.83×10^{-4}
	0.5	1.51×10^{-9}	9.17×10^{-4}
	1 (nominal)	2.21×10^{-9}	1.16×10^{-3}
	2	2.67×10^{-9}	1.32×10^{-3}
	5	3.01×10^{-9}	1.44×10^{-3}
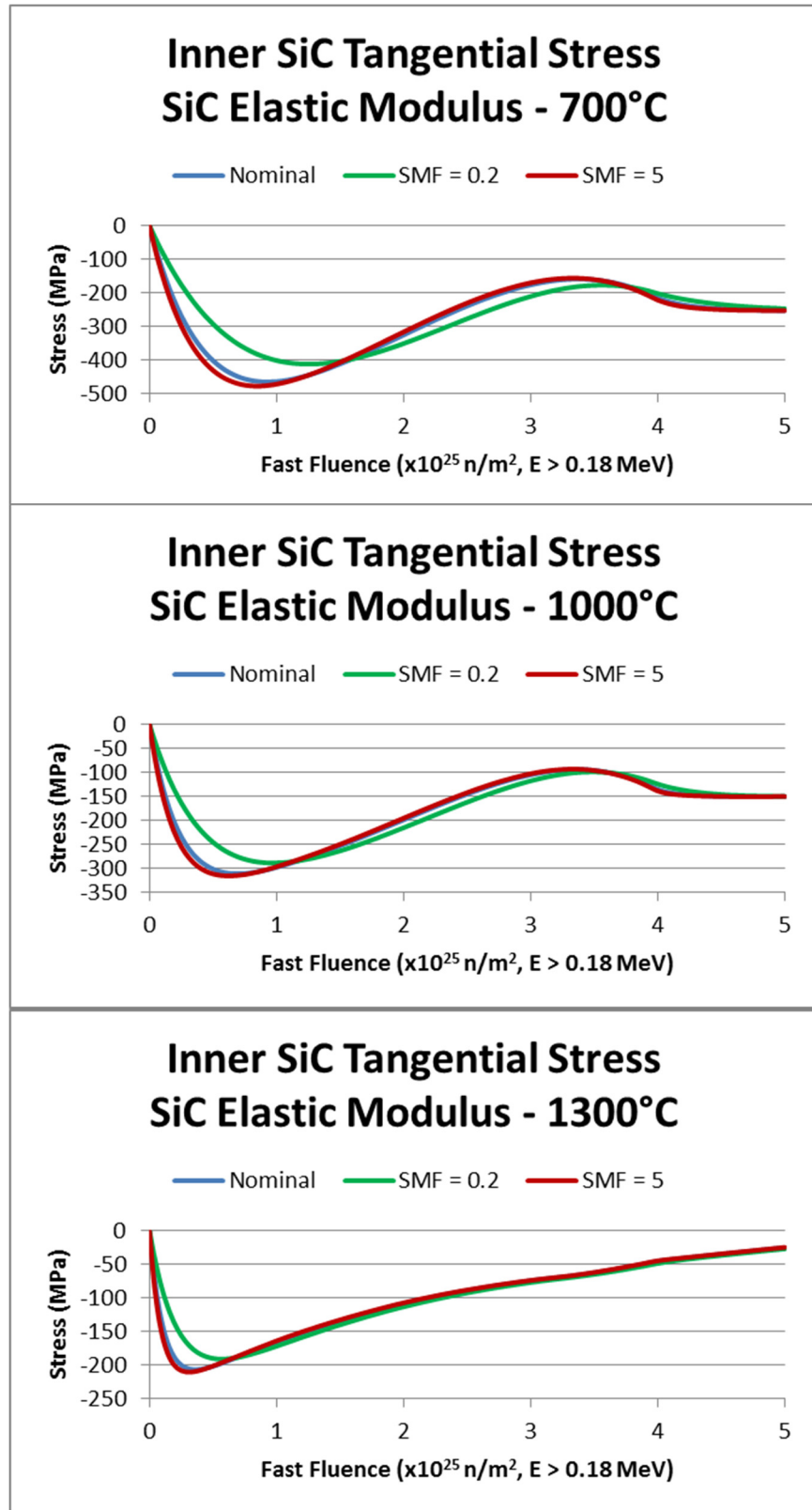
Figure 23. Tangential stress at the inner surface of the SiC layer for the nominal SiC elastic modulus and SMF 0.2 and 5.
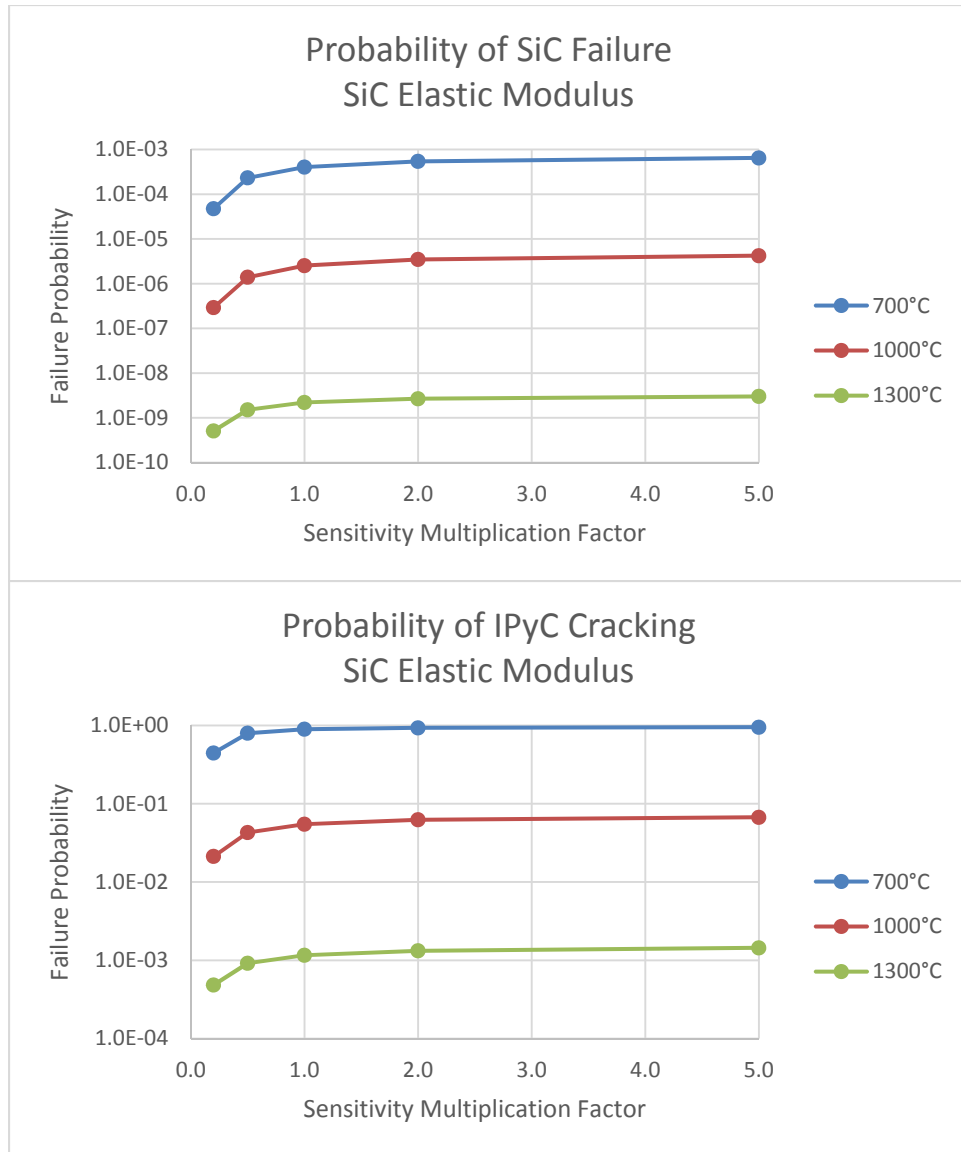
Figure 24. Probability of SiC failure and IPyC cracking as a function of the sensitivity multiplication factor applied to the SiC modulus of elasticity.

Figure 25. Relative difference between the probability of SiC failure and IPyC cracking values and their nominal values as a function of the sensitivity multiplication factor applied to the SiC elastic modulus.

8.2 Poisson's Ratio

The Poisson's ratio of the SiC (μ) is given by:

$\mu = 0.13$

The dependency of the SiC Poisson's ratio on density, fast fluence, and temperature is largely unknown. Therefore, the Poisson's ratio is assumed independent of these parameters and kept at a constant value of 0.13 throughout irradiation, which is consistent with the value provided in the CEGA report.

Review of literature

Yavuz and Tressler (1992) report an identical value of 0.13 for the SiC Poisson's ratio. Additionally, by definition and assuming expansion in the transverse direction under compression in the longitudinal one, the Poisson's ratio ranges from 0 to 0.5.

Range of variation

Overall range of variation: 0–0.5

PARFUME value: 0.13

Sensitivity study

Assuming values of the Poisson's ratio between 0 and 0.5, Table 22 shows its impact on the failure probability of TRISO fuel under the irradiation conditions of Table 1. Figure 26 shows the tangential stress at the inner surface of the SiC layer for the nominal SiC Poisson's ratio and extremum values 0 and 0.5.

Figure 26 and Table 22 show that an increase of the SiC Poisson's ratio and a decrease in temperature increases the compressive stress in the SiC layer and the probabilities of IPyC cracking and SiC failure. This is primarily due to the influence the SiC Poisson's ratio has on the multidimensional effect associated with IPyC cracking. These trends can be seen in Figure 27, which plots the results of Table 22.

Figure 28 shows the relative difference between the probabilities of Table 22 and the nominal probabilities of Table 3. It shows that the probability of SiC failure changes modestly when the Poisson's ratio of SiC is increased to its maximum value of 0.5.

Table 22. Failure probability: SiC Poisson's ratio.

| Condition	Poisson's ratio	Probability of SiC failure	Probability of IPyC cracking
1	0	3.34×10^{-4}	8.83×10^{-1}
	0.13 (nominal)	4.03×10^{-4}	8.94×10^{-1}
	0.25	5.07×10^{-4}	9.04×10^{-1}
	0.5	1.03×10^{-3}	9.23×10^{-1}
2	0	2.04×10^{-6}	5.29×10^{-2}
	0.13 (nominal)	2.52×10^{-6}	5.48×10^{-2}
	0.25	3.23×10^{-6}	5.66×10^{-2}
	0.5	6.79×10^{-6}	6.01×10^{-2}
3	0	1.81×10^{-9}	1.13×10^{-3}
	0.13 (nominal)	2.21×10^{-9}	1.16×10^{-3}
	0.25	2.79×10^{-9}	1.20×10^{-3}
	0.5	5.67×10^{-9}	1.28×10^{-3}
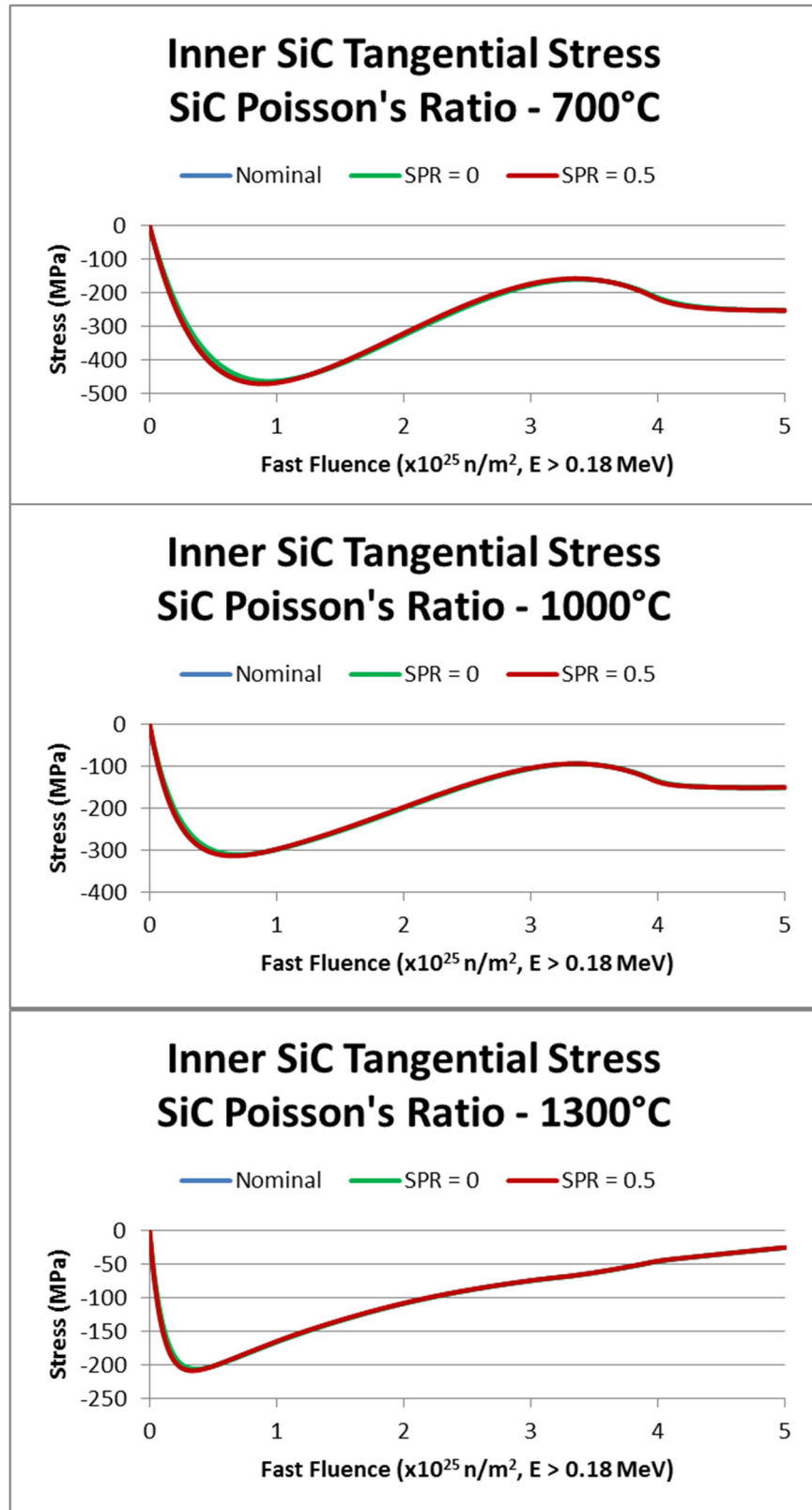
Figure 26. Tangential stress at the inner surface of the SiC layer for the nominal SiC Poisson's ratio and values 0 and 0.5.
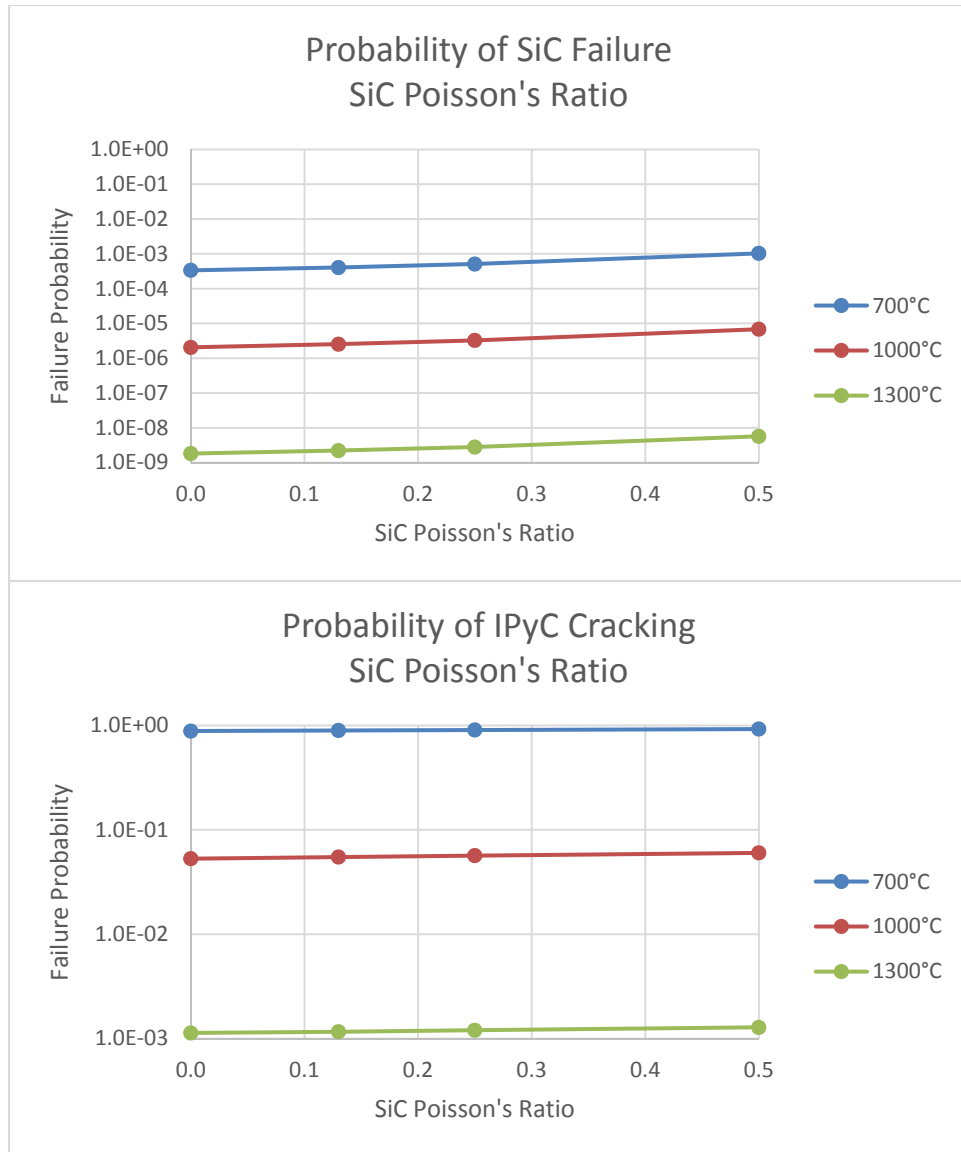
Figure 27. Probability of SiC failure and IPyC cracking as a function of the sensitivity multiplication factor applied to the value of the SiC Poisson's ratio.
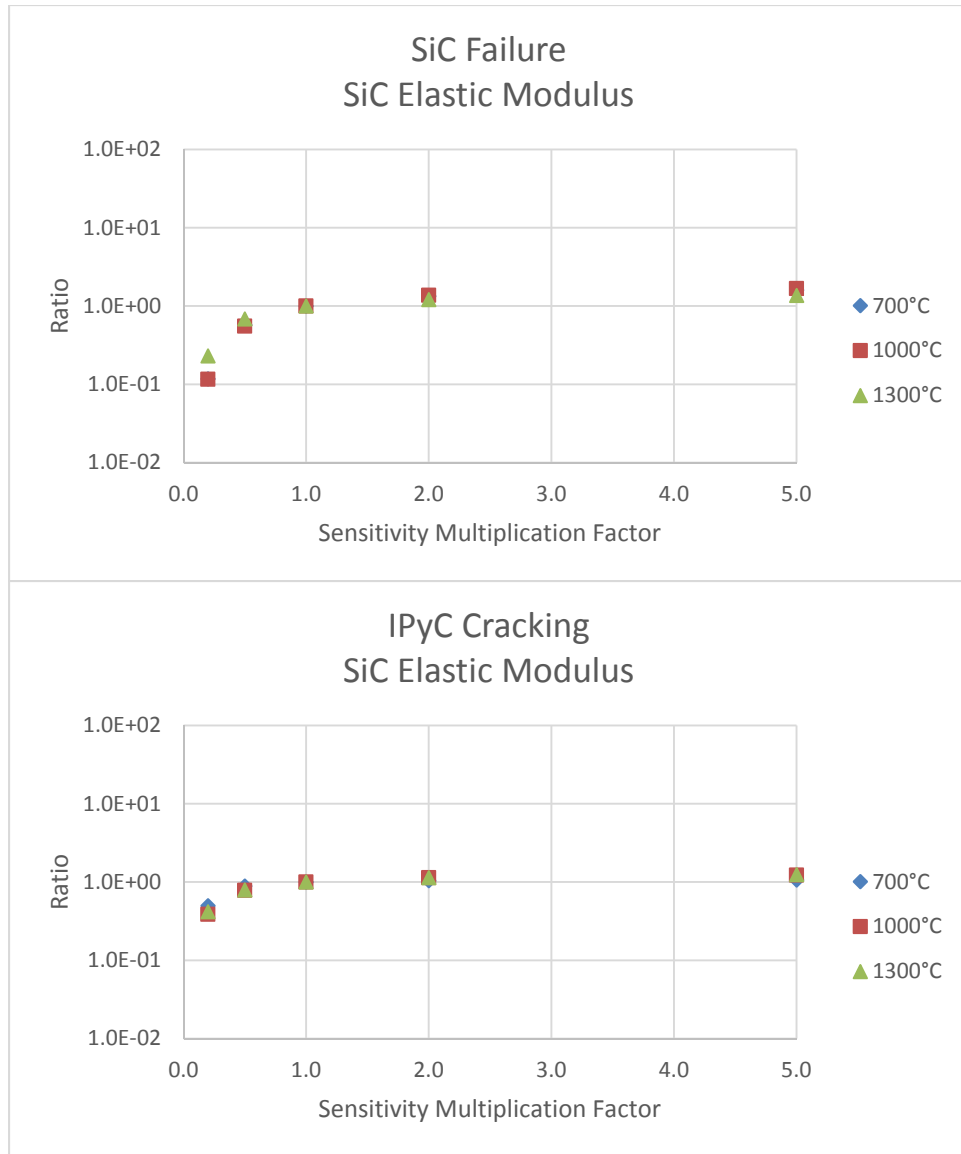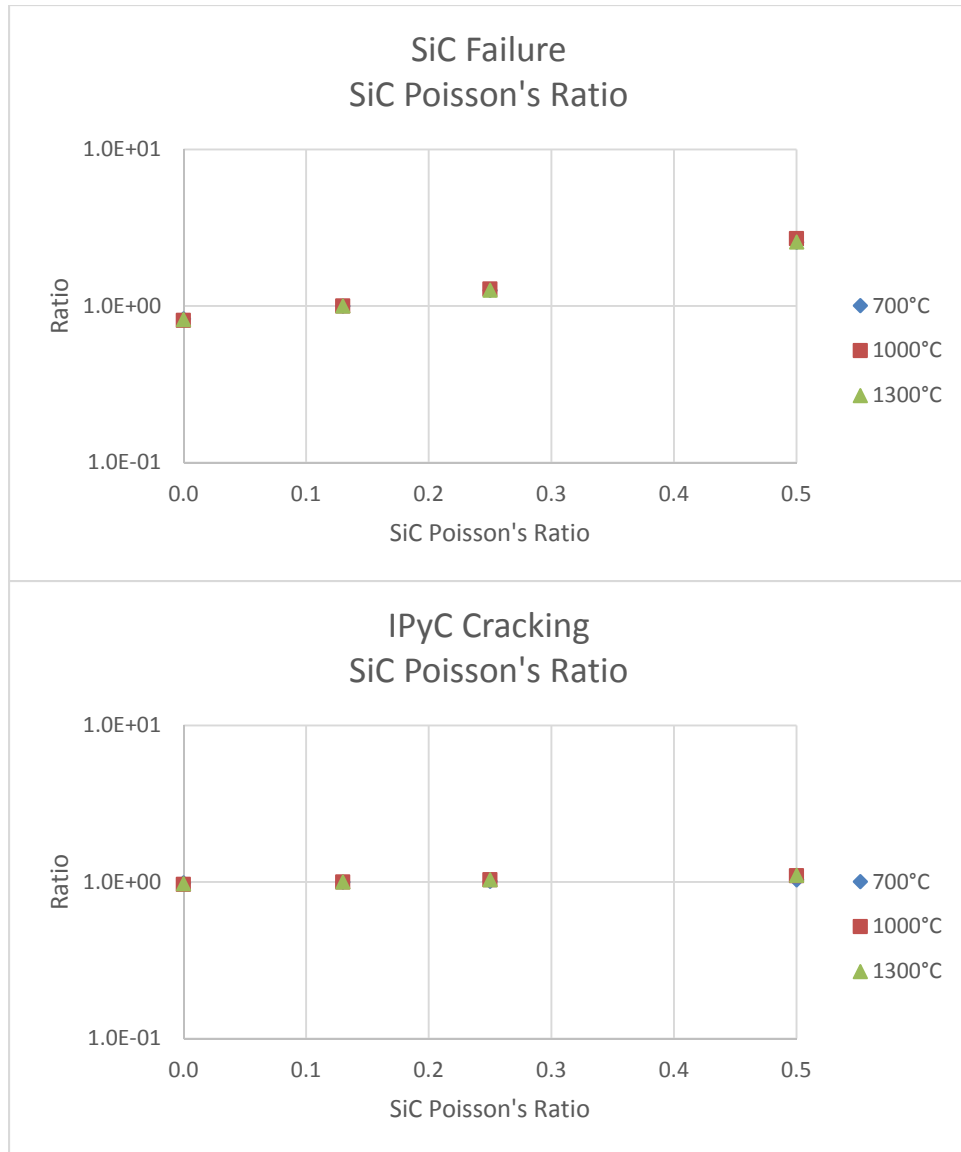
Figure 28. Ratio between the probability of SiC failure and IPyC cracking values and their nominal values as a function of the sensitivity multiplication factor applied to the SiC Poisson's ratio.

8.3 Weibull characteristic strength and modulus

The Weibull characteristic strength (σ_0) and Weibull modulus (m) of the SiC are given by:

$\sigma_0 = 9.64$ MPa-m$^{3/m}$
m = 6

The SiC Weibull parameters are described in the CEGA report. In PARFUME, the SiC Weibull modulus and SiC characteristic strength are assumed to remain constant throughout irradiation and independent of temperature or fast fluence. It is important to note the impact the SiC strength has on fuel particle failure probability since the tensile stress in the SiC layer is compared to the strength to determine particle failure.

Review of literature

The CEGA report indicates that the value of the SiC Weibull modulus varies widely in the literature, from 2 to 9.4. Furthermore, it recommends increasing the modulus by a factor of two at temperatures higher than 1250°C and indicates a decrease of both parameters with fast fluence, although inconsistencies in the available data lead to assuming no irradiation effect on SiC strength. The CEGA report determined the associated SiC characteristic strengths: 9.64 MPa-m$^{3/6}$ and 37.58 MPa-m$^{3/9}$.

A broad review by Snead et al., suggests a large variability in both Weibull modulus and characteristic strength depending on the nature of the sample (bulk SiC, tubes, particles), the potential for free silicon in the SiC, and the test method. The modulus can vary between 3 and 14 and the characteristic strength can vary from 200 to 2200 MPa. Using a modulus of 4 and a mean strength of 250 MPa based on Snead et al., the corresponding characteristic strength was calculated using the following equation (PARFUME Theory Manual and Basis Report):

$$\sigma_{ms} = \sigma_0 / I_n^{1/m}$$

where m is the Weibull modulus and I_n is the normalized integration of the stress distribution over the volume of the SiC layer (μm^3). This resulted in a characteristic strength of 760 MPa.

Range of variation

Overall range of variation: $m = 4$ and $\sigma_0 = 0.76$ MPa-m$^{3/m}$, 6/9.64 MPa-m$^{3/m}$, and 9/37.58 MPa-m$^{3/m}$

PARFUME values: $m = 6$ and $\sigma_0 = 9.64$ MPa-m$^{3/m}$

Sensitivity study

Assuming SiC Weibull moduli of 4, 6, and 9, the corresponding values of the SiC characteristic strength are 0.76 MPa-m$^{3/m}$, 9.64 MPa-m$^{3/m}$, and 37.58 MPa-m$^{3/m}$, respectively. Table 23 shows the impact of the variation of the SiC Weibull parameters on the failure probability of TRISO fuel under the irradiation conditions of Table 1.

Figure 29 shows the probability of SiC failure as a function of the SiC Weibull modulus using results from Table 23.

Figure 30 shows the ratio of the probabilities of SiC failure of Table 23 to the nominal probabilities of Table 3. It shows that the probability of SiC failure drastically decreases when the SiC Weibull parameters are increased at high irradiation temperature. The impact of an increase of the SiC Weibull parameters decreases at lower irradiation temperatures.

Table 23. Failure probability: SiC Weibull parameters.

Condition	Weibull m / σ_0	Probability of SiC failure	Probability of IPyC cracking
1	4 / 0.76	4.99×10^{-3}	8.94×10^{-1}
	6 / 9.64 (nominal)	4.03×10^{-4}	8.94×10^{-1}
	9 / 37.58	1.01×10^{-5}	8.94×10^{-1}
2	4 / 0.76	6.67×10^{-5}	5.48×10^{-2}
	6 / 9.64 (nominal)	2.52×10^{-6}	5.48×10^{-2}
	9 / 37.58	2.03×10^{-8}	5.48×10^{-2}
3	4 / 0.76	1.68×10^{-7}	1.16×10^{-3}
	6 / 9.64 (nominal)	2.21×10^{-9}	1.16×10^{-3}
	9 / 37.58	3.67×10^{-12}	1.16×10^{-3}
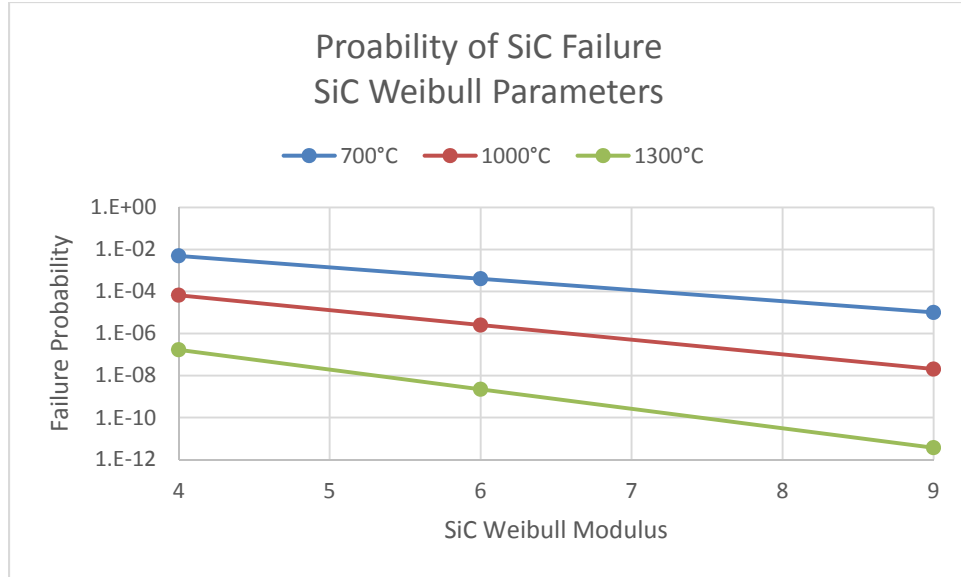
Figure 29. Probability of SiC failure as a function of the SiC Weibull modulus. Each SiC Weibull modulus corresponds the SiC characteristic strength shown in Table 23.
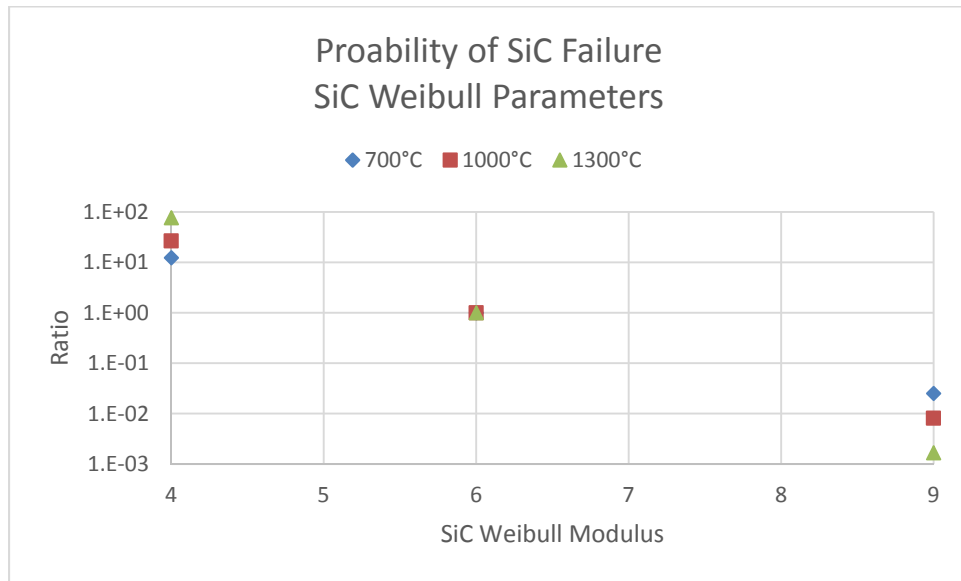
Figure 30. Ratio of the probability of SiC failure values and their nominal values as a function of the SiC Weibull modulus. Each SiC Weibull modulus corresponds the SiC characteristic strength shown in Table 23.

8.4   Thermal Conductivity

The thermal conductivity of the SiC (k) is given by (Nabielek,, et al.):

$$k = \frac{17885}{T+273} + 2 \qquad W/(m \cdot K), \text{ T in } °C$$

The thermal conductivity of the SiC layer decreases with temperature. In these calculations, it varies between 13 and 20 W/(m·K).

Review of literature

The CEA model has a larger range of variation for the SiC thermal conductivity between 700 and 1300°C, with values dropping from about 38 W/(m·K) to about 7 W/(m·K) when taking irradiation effects into account (I-NERI, 2004). Price (1973) gives a thermal conductivity of ~65 W/(m·K) at room temperature, decreasing to ~35 W/(m·K) at 700°C, and to ~10 and ~20 W/(m·K) for irradiated SiC at 550 and 1100°C, respectively. Price (1977) reports thermal conductivities in the range 30–70 W/(m·K) at room temperature, decreasing to 20–30 W/(m·K) at 1200°C, and ~15 W/(m·K) for irradiated SiC at 1200°C. Salgado et al. (1971) suggest a value of 17 W/(m·K). Snead et al. (2007) compiled thermal conductivities that range from ~10 to ~110 W/(m·K) between 700 and 1300°C. A higher value of 168 W/(m·K) is obtained by Lopez-Honorato et al. (2008b).

Range of variation

Overall range of variation: 7–168 W/(m·K)
PARFUME range: 13–20 W/(m·K)

Sensitivity study

Applying SMF to the thermal conductivity of the SiC, Table 24 shows its impact on the failure probability of TRISO fuel under the irradiation conditions of Table 1. Results from Table 24 show that variations of the SiC thermal conductivity have negligible impact on the probability of SiC failure.

Table 24. Failure probability: SiC thermal conductivity.

Condition	Sensitivity Multiplication Factor	Probability of SiC failure	Probability of IPyC cracking
1	0.1	4.03×10^{-4}	8.93×10^{-1}
	0.33	4.03×10^{-4}	8.94×10^{-1}
	1 (nominal)	4.03×10^{-4}	8.94×10^{-1}
	3	4.04×10^{-4}	8.94×10^{-1}
	10	4.04×10^{-4}	8.94×10^{-1}
2	0.1	2.47×10^{-6}	5.37×10^{-2}
	0.33	2.51×10^{-6}	5.45×10^{-2}
	1 (nominal)	2.52×10^{-6}	5.48×10^{-2}
	3	2.52×10^{-6}	5.48×10^{-2}
	10	2.52×10^{-6}	5.49×10^{-2}
3	0.1	2.17×10^{-9}	1.15×10^{-3}
	0.33	2.20×10^{-9}	1.16×10^{-3}
	1 (nominal)	2.21×10^{-9}	1.16×10^{-3}
	3	2.21×10^{-9}	1.17×10^{-3}
	10	2.21×10^{-9}	1.17×10^{-3}

8.5   Thermal Expansion

The thermal expansion coefficient of the SiC (α) is given by:

$$\alpha = 4.9 \qquad \times 10^{-6}/°C$$

The coefficient of thermal expansion of the SiC in PARFUME is taken from Price (1977) and is constant and equal to $4.9 \times 10^{-6}/°C$.

Review of literature

Snead et al. (2007) suggest values varying from 4.9 to $5.0 \times 10^{-6}/°C$ between 700 and 1300°C while CEA reports a variation from 4.4 to $4.8 \times 10^{-6}/°C$ in the same temperature range (I-NERI, 2004).

Range of variation

Overall range of variation: $4.4–5.0 \times 10^{-6}/°C$

PARFUME value: $4.9 \times 10^{-6}/°C$

Sensitivity study

Applying SMFs for the thermal expansion of the PyC in PARFUME, Table 25 shows its impact on the failure probability of TRISO fuel under the irradiation conditions of Table 1. Results show that variations of the SiC thermal expansion have no impact on the probability of SiC failure. Thermal expansion of the SiC layer affects the TRISO particle only if there are non-negligible temperature changes in this layer throughout irradiation, which is not the case in this study, even though typical temperature variations of a few hundred degrees would yield limited thermal expansion with no appreciable impact on the failure probability of the SiC layer.

Table 25. Failure probability: SiC thermal expansion.

Condition	Sensitivity Multiplication Factor	Probability of SiC failure	Probability of IPyC cracking
1	0.5	4.03×10^{-4}	8.94×10^{-1}
	0.66	4.03×10^{-4}	8.94×10^{-1}
	1 (nominal)	4.03×10^{-4}	8.94×10^{-1}
	1.5	4.04×10^{-4}	8.94×10^{-1}
	2	4.04×10^{-4}	8.94×10^{-1}
2	0.5	2.52×10^{-6}	5.47×10^{-2}
	0.66	2.52×10^{-6}	5.47×10^{-2}
	1 (nominal)	2.52×10^{-6}	5.48×10^{-2}
	1.5	2.52×10^{-6}	5.48×10^{-2}
	2	2.52×10^{-6}	5.48×10^{-2}
3	0.5	2.21×10^{-9}	1.16×10^{-3}
	0.66	2.21×10^{-9}	1.16×10^{-3}
	1 (nominal)	2.21×10^{-9}	1.16×10^{-3}
	1.5	2.21×10^{-9}	1.16×10^{-3}
	2	2.21×10^{-9}	1.17×10^{-3}

8.6   Summary of the Material Properties of the SiC Layer

The material properties of the SiC layer used in PARFUME are

- Elastic modulus
- Poisson's ratio
- Weibull characteristic strength and modulus
- Thermal conductivity
- Thermal expansion.

Values reported in the literature for some of the material properties of the SiC layer (elastic modulus, Weibull parameters, and thermal conductivity) show large variability but this has limited impact on the failure probability of that layer. Only changes in the Weibull characteristic strength have significant impact on failure probabilities.

9. SUMMARY

The following section gives a summary of the impact of the material properties on the probability of particle failure in PARFUME modeling.

Properties with no impact

These properties are found not to impact the probability of particle failure:

- Kernel swelling rate
- Kernel thermal conductivity
- Buffer elastic modulus
- Buffer Poisson's ratio
- Buffer irradiation-induced creep
- Buffer Poisson's ratio in creep
- Buffer irradiation-induced dimensional change
- Buffer thermal conductivity
- Buffer thermal expansion
- PyC thermal conductivity
- PyC thermal expansion
- SiC thermal conductivity
- SiC thermal expansion.

Properties with impact

Table 26 shows the material properties for which variations have an impact on the failure probability of the SiC layer, and the table indicates the magnitude of this impact in the case of the most penalizing sensitivity multiplication factor or material property value.

The two main properties that impact the SiC failure probability are the PyC irradiation-induced creep and strain (dimensional change). Their effects on the stress in the SiC layer are in opposite directions: the shrinkage (strain) of the PyC layers puts them into tension and the SiC layer into compression but the creep relieves that tensile stress and reduces somewhat the compressive stress in the SiC layer. Therefore, an increase of the irradiation-induced PyC strain or a decrease of the irradiation-induced PyC creep creates additional tensile stress in the SiC layer, increasing its probability of failure. The failure probability of the SiC layer is sensitive to changes in the irradiation-induced strain and creep of the PyC: an increase in strain or decrease in creep by a factor 2 yields an increase of the SiC failure probability by about two orders of magnitude. In addition, the lower SiC Weibull parameters showed an increase in failure probability by a factor as much as 76 at 1300°C. Increasing the Weibull modulus and corresponding characteristic strength can significantly reduce fuel particle failure probability. To a lesser extent, the PyC Weibull parameters, that drive the calculation of the failure probability, the PyC elastic moduli, and the SiC Poisson's ratio can have a non-negligible impact and increase the failure probability by a factor up to 4.

Table 26. Summary of the maximum impact of material properties on SiC failure probability.

Material Property	Sensitivity Multiplication Factor or Material Property Value	Irradiation Temperature (°C)	Increase in SiC failure probability	SiC failure probability
PyC elastic moduli	× 3	700	1.6	6.54×10^{-4}
		1000	2.7	6.84×10^{-6}
		1300	2.0	4.47×10^{-9}
PyC Poisson's ratio	0.5	700	1.3	5.04×10^{-4}
		1000	1.6	3.96×10^{-6}
		1300	1.4	3.03×10^{-9}
PyC irradiation-induced creep	× 0.2	700	1.1	2.48×10^{-1}
		1000	2.2×10^{4}	5.57×10^{-2}
		1300	3.4×10^{6}	7.50×10^{-3}
PyC Poisson's ratio in creep	Failure probability is maximum at nominal Poisson's ratio in creep			
PyC irradiation-induced dimensional change	× 5	700	2.4×10^{3}	9.68×10^{-1}
		1000	1.7×10^{5}	4.21×10^{-1}
		1300	1.1×10^{7}	2.48×10^{-2}
PyC Weibull parameters (m / σ_0)	8/10.0	700	1.04	4.20×10^{-4}
		1000	2.1	5.37×10^{-5}
		1300	4.1	9.02×10^{-9}
SiC elastic modulus	× 5	700	1.6	6.45×10^{-4}
		1000	1.7	4.21×10^{-6}
		1300	1.4	3.01×10^{-9}
SiC Poisson's ratio	0.5	700	2.6	1.03×10^{-3}
		1000	2.7	6.79×10^{-6}
		1300	2.6	5.67×10^{-9}
SiC Weibull parameters	4 / 0.76	700	12.4	4.99×10^{-3}
		1000	26.5	4.03×10^{-4}
		1300	76.3	1.01×10^{-5}

10. REFERENCES

Abaqus/Standard, "Abaqus User's Manual," Version 6.7, 2007.

Bellan, C., and J. Dhers, "Evaluation of Young modulus of CVD coatings by different techniques," *Thin Solid Films* 469–470 (2014) 214–220.

Booth, A.H., *A method of calculating fission gas diffusion from UO$_2$ fuel and its application to the X-2-f loop test*," Atomic Energy of Canada Limited, AECL-496, September 1957.

Bower, G.R. et al., "Measurement of kernel swelling and buffer densification in irradiated UCO-TRISO particles," *Journal of Nuclear Materials* 486 (2017) 339-349.

Buckley, S.N. et al., "Some estimates of the irradiation creep constant of pyrocarbon contained in the coatings of reactor fuel particles," *12th Biennial Conference of the American Carbon Society, Pittsburgh, PA, 1975*.

CEGA, *NP-MHTGR material models of pyrocarbon and pyrolytic silicon carbide*, Combustion Engineering General Atomics Corporation, CEGA-002820, Rev. 1, July 1993.

Demkowicz, P.A. et al., "Irradiation performance of AGR-1 high temperature reactor fuel," *Nuclear Engineering and Design* 306 (2016) 2-13.

Freis, D., "Accident simulations and post-irradiation investigations on spherical fuel elements for high temperature reactors," Doctoral Dissertation, 2009.

Gulden, T.D., "Mechanical Properties of Polycrystalline β-SiC," *Journal of the American Ceramic Society* 52 (1969) 585-590.

Harding, J.H. and D.G. Martin , "A recommendation for the thermal conductivity of UO$_2$," *Journal of Nuclear Materials* 166 (1989) 223-226.

Hofmann, G. et al., "An investigation of the relationship between position within coater and pyrolytic carbon characteristics using nanoindentation," *Carbon* 38 (2000) 645–653.

Hosemann, P. et al., "Mechanical characteristics of SiC coating layer in TRISO fuel particles," *Journal of Nuclear Materials* 442 (2013) 133-142.

I-NERI., *Development of Improved Models and Designs for Coated-Particle Gas Reactor Fuels*, Idaho National Laboratory, INEEL/EXT-05-02615, December 2004.

INL, "Technical Program Plan for INL Advanced Reactor Technologies Technology Development Office/Advanced Gas Reactor Fuel Development and Qualification Program," Idaho National Laboratory, PLN-3636, Rev. 6, June 2017.

Kaae, J.L. et al., "The mechanical behavior of BISO-coated fuel particles during irradiation. Part II: prediction of BISO particle behavior during irradiation with a stress-analysis model," *Nuclear Technology* 35 (1977) 359-378.

Kaae, J.L., "Calculation of irradiation-induced stresses in restrained pyrolytic carbons," Physical Metallurgy of Reactor Fuel Elements, *The Metals Society*, London, UK, 1973.

Kaae, J.L., "On irradiation-induced creep of pyrolytic carbon in a general state of stress," *Journal of Nuclear Materials* 34 (1970) 206-208.

Kaae, J.L., "Relations between the structure and the mechanical properties of fluidized-bed pyrolytic carbons," *Carbon* 9 (1971) 291-299.

Lopez-Honorato, E. et al., "Structure and mechanical properties of pyrolytic carbon produced by fluidized bed chemical vapor deposition," *Nuclear Engineering and Design* (2008a) 3121-3128.

Lopez-Honorato, E. et al., "Thermal conductivity mapping of pyrolytic carbon and silicon carbide coatings on simulated fuel particles by time-domain thermoreflectance," *Journal of Nuclear Materials* 378 (2008b) 35-39.

Marshall, D.W., "AGR-5/6/7 Fuel Specification," Idaho National Laboratory, SPC-1352, Rev. 8, March 2017.

Martin, D.G., "Considerations pertaining to the achievement of high burn-ups in HTR fuel," *Nuclear Engineering and Design* 213 (2002) 241-258.

Miller, G.K. and D.C. Wadsworth, "Treating asphericity in fuel particle pressure vessel modeling," *Journal of Nuclear Materials* 211 (1994) 57-69.

Miller, G.K. et al., "Statistical approach and benchmarking for modeling of multi-dimensional behavior in TRISO-coated fuel particles," *Journal of Nuclear Materials* 317 (2003) 69-82.

Miller, G.K. et al., *PARFUME Theory and Model Basis Report*, Idaho National Laboratory, INL/EXT-08-14497, September 2009.

Morgand, P., "Fluage du pyrocarbone sous irradiation," *Journal of Nuclear Materials* 58 (1975) 47-54.

Nabielek, H. et al., "Calculation of particle temperatures in NSRR tests," JAERI, unpublished draft from March 13, 1992.

Price, R.J. and J.C. Bokros, "Mechanical properties of neutron-irradiated pyrolytic carbons," *Journal of Nuclear Materials* 21 (1967) 158-174.

Price, R.J. and J.L. Kaae, "Poisson's Ratio of Pyrolytic Carbon," *Carbon* 7 (1969) 706-708.

Price, R.J., "Properties of silicon carbide for nuclear fuel particle coatings," *Nuclear Technology* 35 (1977) 320-336.

Price, R.J., "Thermal conductivity of neutron-irradiated pyrolytic β-silicon carbide," *Journal of Nuclear Materials* 46 (1973) 268-272.

Rochais, D. et al., "Microscopic thermal characterization of HTR particle layers," *Nuclear Engineering and Design* 238 (2008) 3047-3059.

Ronchi, C. et al., "Thermal conductivity of uranium dioxide up to 2900 K from simultaneous measurement of the heat capacity and thermal diffusivity," *Journal of Applied Physics* 85 (1999) 776-789.

Salgado, P.G. et al, "Determination of Pyrocarbon Thermal Conductivity by the Burst-Reactor Technique," *Nuclear Technology* 11 (1971) 131-143.

Siefken, L.J. et al., "SCDAP/RELAP5/MOD3.3 Code Manual: MATPRO – A Library of Materials Properties for Light-Water-Reactor Accident Analysis," Nuclear Regulatory Commission, NUREG/CR-6150, Vol. 4, Rev. 2, January 2001.

Snead, L.L. et al., "Handbook of SiC properties for fuel performance modeling," *Journal of Nuclear Materials* 371 (2007) 329-377.

Yavuz, B.O. and R.E. Tressler, "High Temperature Mechanical Behavior of a Chemically Vapor Deposited Beta Silicon Carbide," *Ceramics International* 18 (1992) 19-26.